

LAYER-BY-LAYER DEPOSITION OF GRAFTED PHEMA-*g*-PAA/PAH  
POLYELECTROLYTE MULTILAYER FILMS AND LYSOZYME BINDING

By

Yiding Ma

A THESIS

Submitted to  
Michigan State University  
in partial fulfillment of the requirements  
for the degree of

MASTER OF SCIENCE

Chemistry

2011

## ABSTRACT

### LAYER-BY-LAYER DEPOSITION OF GRAFTED PHEMA-*g*-PAA/PAH POLYELECTROLYTE MULTILAYER FILMS AND LYSOZYME BINDING

By

Yiding Ma

Improving the binding capacity of polyelectrolyte multilayers (PEMs) is important for their application as a platform for protein capture and immobilization. In this work, we aimed to create PEMs from comb-like poly(2-hydroxyethyl methacrylate)-*graft*-poly(acrylic acid) (PHEMA-*g*-PAA) and poly(allyl amine hydrochloride) (PAH), and subsequently adsorb lysozyme throughout the film. At all deposition pH values, the thickness of (PAH/PHEMA-*g*-PAA)<sub>n</sub> films grow faster and more exponential than (PAH/PAA)<sub>n</sub>. In addition, (PAH/PAA)<sub>n</sub> and (PAH/PHEMA-*g*-PAA)<sub>n</sub> films show similar trends in thickness as a function of adsorption pH. The presence of supporting electrolyte in the deposition solutions, 0.5 NaCl, leads to thicker films by varying pH in the absence of salt. Lysozyme binding capacities of (PAH/PHEMA-*g*-PAA)<sub>5</sub> films, deposited at pH values  $\geq 5$ , are 2 to 5 fold higher than the values of corresponding (PAH/PAA)<sub>5</sub> coatings, and (PAH/PHEMA-*g*-PAA)<sub>5</sub> and (PAH/PAA)<sub>5</sub> films deposited from solutions containing 0.5 M NaCl greatly enhances lysozyme adsorption, regardless of the deposition pH. The relatively high lysozyme binding capacity of our new (PAH/PHEMA-*g*-PAA)<sub>n</sub> films provides potential applications of these PEM systems for protein purification or immobilization.

## ACKNOWLEDGMENTS

Firstly, I would like to thank my advisor, Professor Gregory L. Baker, for being a great mentor over the past three years. I really appreciate his kindness, patience and encouragement throughout my graduate study at Michigan State University. His valuable guidance leads me to think as a scientist, and I will benefit from his advice not only for my research in chemistry, but also for my future career and life.

I also want to thank Professor Merlin L. Bruening for his great help on my research. He is an excellent research advisor who thinks critically and has a special attitude for scientific research. I would not have completed this project without his idea and patience. I also want to express my gratitude to my committee member, Dr. Xuefei Huang, who has exceptional knowledge in organic chemistry and gave me useful advice.

I would also like to express gratitude to past and present Baker's group members for their help and suggestions: Sampa, Qin, Gina, Hui, Heyi, Wen, Quanxuan, Greg, Zhe and Salinda. I also enjoyed working with Bruening group members, especially Somnath, Fei, Weihang, Nishotha and Jinlan for their directly involvement in my research project. Thanks to all the faculty and staff in Department of Chemistry for their kindness to me.

Lastly, I express my special gratitude to my parents for all of their support and understanding through the years. And I will never forget my friends at MSU and elsewhere.

## TABLE OF CONTENTS

List of Figures .....	vi
List of Schemes .....	ix
Abbreviations .....	x
Chapter 1. Introduction .....	1
1.1. Organic thin films .....	1
1.2. Layer-by-layer (LbL) deposition of polyelectrolyte multilayers (PEMs).....	2
1.2.1. Mechanism of polyelectrolyte adsorption.....	2
1.2.2. Factors that affect LbL polyelectrolyte adsorption.....	4
1.3. Application of PEMs for binding proteins.....	7
1.4. Grafted copolymers prepared by atom transfer radical polymerization (ATRP).....	10
1.5. Research motivation and objectives.....	12
Chapter 2. Layer-by-layer deposition of PHEMA- <i>g</i> -PAA/PAH bilayers on Au substrates 14	
2.1. Synthesis of PHEMA- <i>g</i> -PAA .....	14
2.2. Formation of (PAH/PHEMA- <i>g</i> -PAA) <sub>n</sub> films .....	18
Chapter 3. Lysozyme Binding on (PAH/PHEMA- <i>g</i> -PAA) <sub>n</sub> and (PAH/PAA) <sub>n</sub> multilayers.....	27
3.1. Lysozyme binding on (PAH/PHEMA- <i>g</i> -PAA) <sub>n</sub> and (PAH/PAA) <sub>n</sub> multilayers deposited at various pH values .....	27
3.2. Lysozyme binding on (PAH/PHEMA- <i>g</i> -PAA) <sub>n</sub> and (PAH/PAA) <sub>n</sub> multilayers deposited with a supporting electrolyte .....	29
3.3. Comparison of lysozyme binding capacities of (PAH/PHEMA- <i>g</i> -PAA) <sub>n</sub> and (PAH/PAA) <sub>n</sub> multilayers .....	31
Chapter 4. Experimental .....	34
4.1. Materials .....	34
4.2. Preparation of poly(2-hydroxyethyl methacrylate)- <i>graft</i> -poly(acrylic acid) (PHEMA- <i>g</i> -PAA) .....	35
4.2.1. ATRP of HEMA .....	35
4.2.2. Preparation of macroinitiator, poly(2-(2-bromoisobutyryloxy)ethyl methacrylate) (PBIEM).....	35
4.2.3. Preparation of PHEMA- <i>g</i> -PtBA .....	36
4.2.4. Hydrolysis of PHEMA- <i>g</i> -PtBA to PHEMA- <i>g</i> -PAA .....	36
4.3. Preparation of polyelectrolyte multilayer (PEM) films .....	36
4.4. Characterization of polymers and PEM films.....	37

4.5. Lysozyme binding.....	38
References .....	40

## LIST OF FIGURES

Figure 1.1.	Layer-by-layer (LbL) deposition of polyelectrolyte multilayers (PEMs). .....2	2
Figure 1.2.	Schematic drawing showing the buildup of a polyelectrolyte “bilayer” during linear growth and exponential growth.....4	4
Figure 1.3.	Growth behavior for PAA/PAA PEMs resulting from charge mismatch. The PAA/PAH charge ratios for increasing pH, expressed as the linear charge density, are (I to V) 4:7, 7:12, 7:6, 7:8, and 7:6. Regions II and IV show exponential growth, while I, III, and V show linear growth. .....6	6
Figure 1.4.	Schematic of protein adsorption onto/into PEMs. Apparent monolayers (a and b), and apparent multilayers (c and d).....9	9
Figure 1.5.	Three main strategies for preparing grafted copolymers. ....10	10
Figure 1.6.	Cross-section of layer-by-layer deposition of (a) linear polymers and (b) grafted polymers. ....13	13
Figure 2.1.	<sup>1</sup> H NMR spectra of (a) PHEMA and (b) PBIEM in CDCl <sub>3</sub> with 10% <i>d</i> <sup>6</sup> -DMSO.....15	15
Figure 2.2.	Gel-permeation chromatograms of (a) PBIEM and (b) PHEMA- <i>g</i> -PtBA detected using a multi-angle light scattering detector.....16	16
Figure 2.3.	Ellipsometric thicknesses of (PAH/PHEMA- <i>g</i> -PAA) <sub>n</sub> (triangles) and (PAH/PAA) <sub>n</sub> films (squares) deposited at pH=7 on Au substrates modified with a monolayer of MPA. The polyelectrolyte deposition solutions contained no NaCl. Integer numbers of bilayers indicate films terminated with PHEMA- <i>g</i> -PAA, and films with an extra half bilayer end in PAH. .....19	19
Figure 2.4.	Ellipsometric thicknesses of (PAH/PHEMA- <i>g</i> -PAA) <sub>5</sub> (triangles) and (PAH/PAA) <sub>5</sub> (squares) films deposited from solutions with various pH values and no supporting electrolyte. The numbers above the triangles represent the ratio of the average thicknesses of the two types of films deposited at the same pH. Data points are average of two trials and error bars here and below represents the difference of two trials.....21	21

Figure 2.5.	Ellipsometric thicknesses of (PAH/PHEMA- <i>g</i> -PAA) <sub>10</sub> or (PAH/PAA) <sub>10</sub> films deposited from polyelectrolyte solutions with various pH values and no supporting electrolyte. Numbers in the figure represent the ratio of the (PAH/PHEMA- <i>g</i> -PAA) <sub>10</sub> and (PAH/PAA) <sub>10</sub> thicknesses. ....	22
Figure 2.6.	Ellipsometric thicknesses of (PAH/PHEMA- <i>g</i> -PAA) <sub>n</sub> films deposited from polyelectrolyte solutions with various pH values and no supporting electrolyte. Integral bilayers indicate films terminated with PHEMA- <i>g</i> -PAA, and films with an extra half bilayer end in PAH. ....	23
Figure 2.7.	Thickness of (PAH/PHEMA- <i>g</i> -PAA) <sub>5</sub> and (PAH/PAA) <sub>5</sub> multilayers deposited from polyelectrolyte solutions containing 0.5 M NaCl at various pH values. The numbers above the triangles represent the ratio of the average thicknesses of the two types of films deposited at the same pH. ....	24
Figure 2.8.	Ellipsometric thicknesses of (PAH/PHEMA- <i>g</i> -PAA) <sub>5</sub> multilayers deposited from polyelectrolyte solutions at various pH values in the presence and absence of 0.5 M NaCl. ....	25
Figure 2.9.	Ellipsometric thicknesses of (PAH/PHEMA- <i>g</i> -PAA) <sub>n</sub> films deposited from polyelectrolyte solutions containing 0.5 M NaCl at various pH values. Integral bilayers indicate films terminated with PHEMA- <i>g</i> -PAA, and half bilayer films end in PAH. Films with more than 5 bilayers layers are relatively rough, so there is significant scatter in the ellipsometric results. ....	26
Figure 3.1.	Film thicknesses and the equivalent thickness of lysozyme sorbed in (PAH/PHEMA- <i>g</i> -PAA) <sub>5</sub> and (PAH/PAA) <sub>5</sub> multilayers deposited from polyelectrolyte solutions with various pH values and no supporting electrolyte. The numbers above the bars represent the ratios of the lysozyme equivalent thickness to the film thickness. The equivalent thickness is the thickness of spin-coated lysozyme that would give an FTIR absorbance equivalent to that of the sorbed lysozyme. ....	29
Figure 3.2.	Film thicknesses and the equivalent thickness of lysozyme sorbed in (PAH/PHEMA- <i>g</i> -PAA) <sub>5</sub> and (PAH/PAA) <sub>5</sub> multilayers deposited from polyelectrolyte solutions containing 0.5 M NaCl at various pH values. The numbers above the bars represent the ratios of the lysozyme equivalent thickness to the film thickness. The equivalent thickness is the thickness of spin-coated lysozyme that would give an FTIR absorbance equivalent to that of the sorbed lysozyme. ....	30

Figure 3.3. Lysozyme binding capacities of (PAH/PHEMA-*g*-PAA)<sub>n</sub> or (PAH/PAA)<sub>n</sub> multilayers (n=1~5) deposited from polyelectrolyte solutions containing 0.5 M NaCl at pH=3. The numbers above the bars represent the ratios of the lysozyme equivalent thickness to the film thickness. The equivalent thickness is the thickness of spin-coated lysozyme that would give an FTIR absorbance equivalent to that of the sorbed lysozyme. ....32

Figure 3.4. Lysozyme binding capacities of (a) (PAH/PHEMA-*g*-PAA)<sub>n</sub> and (b) (PAH/PAA)<sub>n</sub> multilayers (n=1~5) deposited from polyelectrolyte solutions at pH=3 both in the presence and absence of 0.5 M NaCl. The numbers above the bars represent the ratios of the lysozyme equivalent thickness to the film thickness. The equivalent thickness is the thickness of spin-coated lysozyme that would give an FTIR absorbance equivalent to that of the sorbed lysozyme .....33

## LIST OF SCHEMES

Scheme 1.1.	Kinetic scheme of ATRP .....	11
Scheme 2.1.	Synthesis of poly(2-hydroxyethyl methacrylate)- <i>g</i> -poly(acrylic acid) (PHEMA- <i>g</i> -PAA) .....	17

## LIST OF ABBREVIATIONS

A	Absorbance
ATRP	Atom transfer radical polymerization
bpy	2,2-Bipyridine
CRP	Controlled radical polymerization
DMSO	Dimethyl sulfoxide
EBiB	Ethyl 2-bromoisobutyrate
FTIR	Fourier transform infrared
GPC	Gel permeation chromatography
HEMA	2-Hydroxyethyl methacrylate
$I$	Ionic strength
$k_{act}$	Activation rate constant
$k_{deact}$	Deactivation rate constant
$k_p$	Polymerization rate constant
$k_t$	Termination rate constant
LbL	Layer-by-layer
MALL	Multiangle light scattering detector
MEK	Methyl ethyl ketone
MHz	Million Hertz
$M_n$	Number average molecular weight
MPA	Mercaptopropionic acid

$M_w$	Weight average molecular weight
NMP	Nitroxide-mediated polymerization
NMR	Nuclear magnetic resonance
PAA	Poly(acrylic acid)
PAH	Poly(allylamine hydrochloride)
PBIEM	Poly(2-(2-bromoisobutyryloxy)ethyl methacrylate)
PDADMAC	Poly(diallyldimethylammonium chloride)
PEM	Polyelectrolyte multilayer
PHEMA	Poly(2-hydroxyethyl methacrylate)
PHEMA- <i>g</i> -PAA	Poly(2-hydroxyethyl methacrylate)- <i>graft</i> -poly(acrylic acid)
PHEMA- <i>g</i> - <i>Pt</i> BA	Poly(2-hydroxyethyl methacrylate)- <i>graft</i> -poly( <i>tert</i> -butyl acrylate)
PMDETA	N,N,N',N',N''-pentamethyldiethylenetriamine
ppm	Parts-per-million
PSS	Poly(styrene sulfonate)
<i>Pt</i> BA	Poly( <i>tert</i> -butyl acrylate)
RAFT	Reversible addition-fragmentation chain transfer
SAM	Self-assembled monolayer
<i>t</i> BA	<i>tert</i> -Butyl acrylate
THF	Tetrahydrofuran
UV	Ultraviolet

# Chapter 1

## Introduction

### 1.1. Organic thin films

Thin films of organic compounds on solid substrates have a variety of potential applications as antibacterial or biocompatible coatings, substrates that capture or immobilize proteins, and selective membrane skins for nanofiltration or gas separation.<sup>1-3</sup> Techniques for preparation of organic thin films have been developed for a long time including spin coating, Langmuir-Blodgett assembly and adsorption of self-assembled monolayers (SAMs). However, these classical techniques have significant limitations such as the need for special equipment, specific functional groups in film-forming molecules, and restrictions with regard to substrate topology and chemical compositions. In the last 20 years, the growth of polymer brushes<sup>2,4-6</sup> and layer-by-layer (LbL) deposition of complementary polymers<sup>7-15</sup> have emerged as versatile tools for forming a wide range of stable, thin films on many types of substrates including 3-dimensional structures such as porous membranes.<sup>3</sup> The growth of polymer brushes often produce films with high grafting densities and thicknesses, and provides accurate control over chemical composition and architecture.<sup>2</sup> However, this process requires both initiator immobilization and polymerization under controlled conditions with a high concentration of monomer. The next section discusses the main focus of this thesis, layer-by-layer deposition, which also has assets and limitations.

## 1.2. Layer-by-layer (LbL) deposition of polyelectrolyte multilayers (PEMs)

Decher and co-workers<sup>14</sup> popularized LbL deposition in the 1990s. This technique simply includes alternating immersion of a substrate into polycation and polyanion solutions along with rinsing steps (Figure 1.1).<sup>13</sup> LbL adsorption can occur on a wide range of substrates, including flat surfaces, nanoparticles<sup>16-19</sup> and membranes.<sup>20-25</sup> Furthermore, a variety of charged molecules, including colloids and biomacromolecules, can serve as the polyelectrolytes in LbL films. Unfortunately, LbL deposition has the inherent drawback of multiple processing steps. Although new spray methods may overcome this challenge to some extent,<sup>26-31</sup> this is a major challenge for large-scale, low-cost applications.

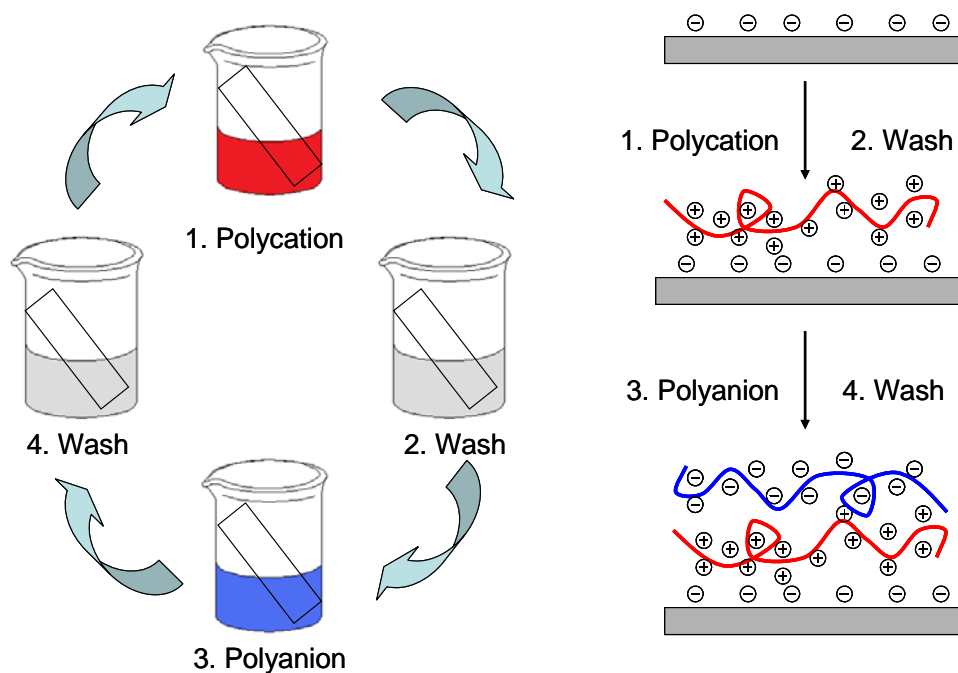


**Figure 1.1** Layer-by-layer (LbL) deposition of polyelectrolyte multilayers (PEMs).<sup>13</sup> For interpretation of the references to color in this and all other figures, the reader is referred to the electronic version of this thesis.

### 1.2.1. Mechanism of polyelectrolyte adsorption

The driving force for adsorption can arise from electrostatic interactions that displace

counterions on the surface to increase entropy,<sup>32</sup> as well as non-electrostatic interactions, such as van der Waals forces, charge-transfer halogen interactions,<sup>33</sup> hydrogen bonds<sup>34</sup> and hydrophobic effects.<sup>35</sup> Two growth modes of PEMs are investigated: linear and exponential. Some systems showed linear increases in film thickness with the number of layers deposited, e.g. poly(styrene sulfonate)/ poly(allylamine hydrochloride) (PSS/PAH) films.<sup>36-37</sup> This suggests that each polyelectrolyte layer interpenetrates only its neighboring layers, and the roughness and surface potential remain the same after a full deposition cycle. On the other hand, the film thickness of some polyelectrolyte systems increases exponentially with the number of layers. Polyelectrolyte diffusion 'in' and 'out' of the film was found to be a key feature in film growth. Hoda et al. suggested a theoretical model for exponential growth, which features polyelectrolyte diffusion 'in' and 'out' of the film during deposition.<sup>38</sup> One of the mobile polyelectrolytes, with low charge density and high swelling in water, diffuse into the films to balance the chemical potential. Upon addition of the oppositely charged polyelectrolyte, this mobile polyelectrolyte diffuses out of the entire film to form a polyanion/polycation complex at the surface. These complexes of both types of polyelectrolytes lead to the additional mass and thickness of the multilayer. The number of more mobile polyelectrolyte which can complex with the oppositely charged polyelectrolytes increases with film thickness, thus the increment of film thickness increases with the number of layers, which leads to an exponential growth. It also appears that exponential growth becomes dominant when NaCl concentrations increase<sup>39</sup> or when temperature is increased.<sup>40</sup>

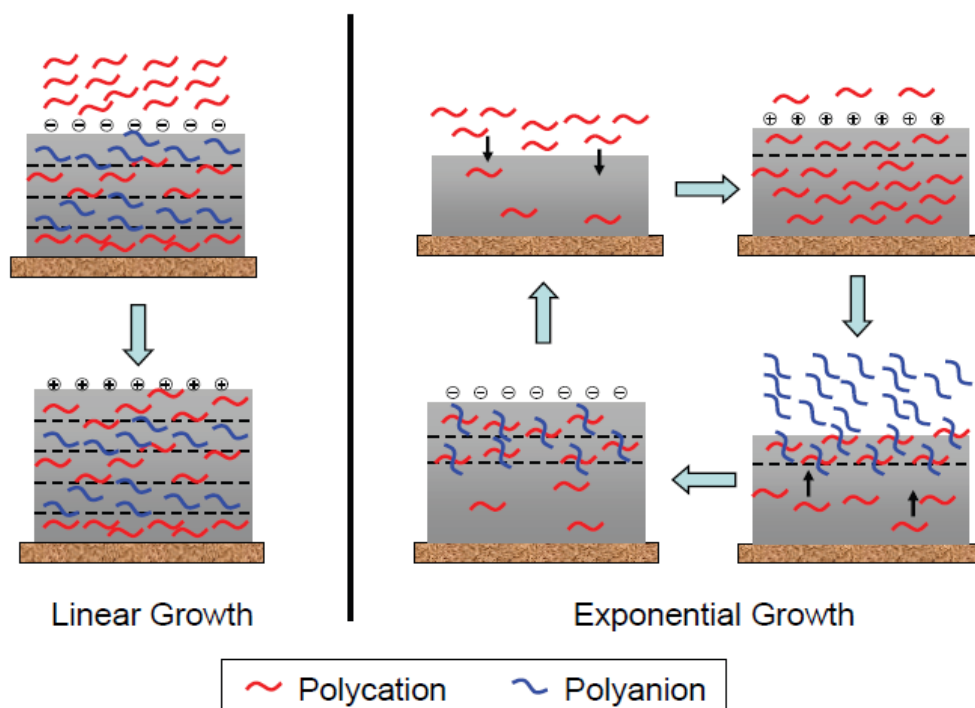


**Figure 1.2** Schematic drawing showing the buildup of a polyelectrolyte “bilayer” during linear growth and exponential growth.<sup>38</sup>

### 1.2.2. Factors that affect LbL polyelectrolyte adsorption

The amount of adsorbed polyelectrolyte and surface structure of PEMs can be controlled by a number of factors. Here we mainly discuss the effect of deposition pH and the supporting electrolyte, which provide simple and effective adjustments of PEMs, especially where one polyelectrolyte is weakly charged. In addition, other adsorption parameters, such as supporting electrolyte concentration and composition,<sup>39,41</sup> molecular weight of the polyelectrolyte,<sup>42-45</sup> adsorption time<sup>41</sup> and temperature,<sup>40,46-47</sup> also influence polyelectrolyte adsorption.

The ionization of weak polyelectrolytes is strongly influenced by the pH value of the solution, resulting in PEMs highly sensitive to the deposited pH.<sup>48-50</sup> Therefore, it is possible to control the properties of multilayers with small changes in solution pH value, such as the

thickness of adsorbed polyelectrolyte, the bulk and surface composition, and charge density on the surface. The mechanism of pH-dependent growth behavior for PAA/PAH multilayers were studied by Shiratori<sup>49</sup> and Bieker,<sup>48</sup> and five distinct pH regimes (3~4.5, 4.5~6, 6~8, 8~10, 10~12) of PAA and PAH solutions were identified. The behavior is symmetric around an intermediate pH in the neutral region (pH 6~8). Both polyions have a similar high charge density and form rigid and thin layers with a linear growth law as they are strong polyelectrolytes. Next to this regime (pH 4.5~6 and 8~10), one of the two polyelectrolytes becomes less charged. Interpenetration of polymer chains is strongly enhanced due to lower electrostatic interactions, resulting in exponential growth and thick layers. At an even higher or lower deposited pH, the larger mismatch of charge density leads to extremely asymmetric layers and a linear growth law.

The supporting electrolyte is another important factor on the growth of PEMs. It is widely reported that additional salt in polyelectrolyte dipping solutions increases the thickness and roughness for various polyanion/polycation systems.<sup>32,39,50</sup> Due to the extrinsic charge compensation of polyelectrolyte and counterions, charges along the polyelectrolyte chains are screened, resulting in coiled conformations and more exponential growth.<sup>51</sup>

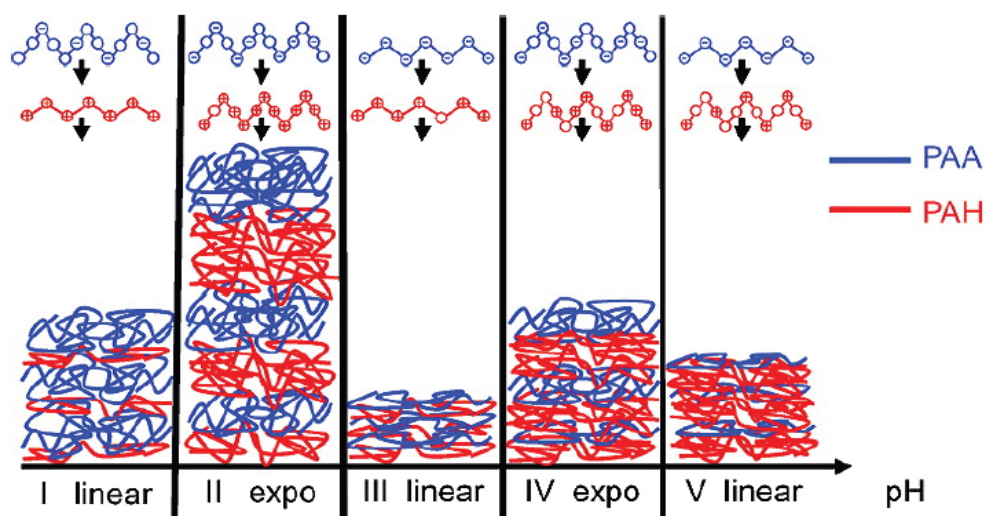


**Figure 1.3** Growth behaviors for PAA/PAH PEMs resulting from charge mismatch. The PAA/PAH charge ratios for increasing pH, expressed as the linear charge density, are (I to V) 4:7, 7:12, 7:6, 7:8, and 7:6. Regions II and IV show exponential growth, while I, III, and V show linear growth.<sup>48</sup> (Reprinted from *Macromolecules* **2010**, *43*, 5052. Copyright 2010 American Chemical Society.)

The supporting electrolyte concentration shows a dramatic effect on the thickness of PEMs. The increase in thickness  $d$  for different polyanion–polycation combinations is proportional to  $I^B$  ( $I$ : ionic strength), and an exponent  $B$  as the salt varies between 0.5 and 1.<sup>51</sup> McAloney *et al.* examined the morphology of multilayer PDADMAC/PSS films deposited from solutions with salt concentrations ranging from  $10^{-4}$  to 1.0 M.<sup>39</sup> Significant differences were observed between films formed under low salt concentrations and those produced under high concentrations. (PDADMAC/PSS)<sub>10</sub> films deposited from solutions with less than 0.3 M added NaCl were flat and featureless, and the thickness increased linearly with the number of adsorbed bilayers, a consequence of the extended rod configuration of the polyelectrolyte. In contrast, PDADMAC/PSS films deposited from an ionic strength of 0.3 M or higher had a vermiculate morphology, and the growth rate and roughness increased. However, very high salt concentrations were reported to dissolve the film.<sup>52</sup>

### 1.3. Application of PEMs for binding proteins

One attractive application of PEM assemblies is embedding bioactive proteins into thin films, and utilizing their unique functions in opto-electrical devices, sensors, drug delivery, cell seeding and growth, tissue engineering, and implantable materials.<sup>9</sup> The simple growth of PEMs on nanostructured substrates is a powerful tool to prepare biological devices.

Adsorption of proteins onto PEMs is attributed to electrostatic forces and non-electrostatic interactions, such as hydrogen bonds, hydrophobic interactions, and hydrophilic repulsion.<sup>53-55</sup> The effects of PEMs surface charge on the adsorption behavior of different types of proteins, including serum albumin, fibrinogen, and lysozyme, have been

studied.<sup>53-58</sup> In these cases, proteins strongly interacted with the PEMs films regardless of the sign of the charges for both the multilayers and the proteins. For like-charged multilayer and proteins, one monolayer of protein adhered on the film because of hydrogen-bonding and hydrophobic interactions. However, the interaction of oppositely charged protein and multilayer is dominated by electrostatic force, thus forming dramatically thicker protein layers which extend up to several times the dimension of the single protein.

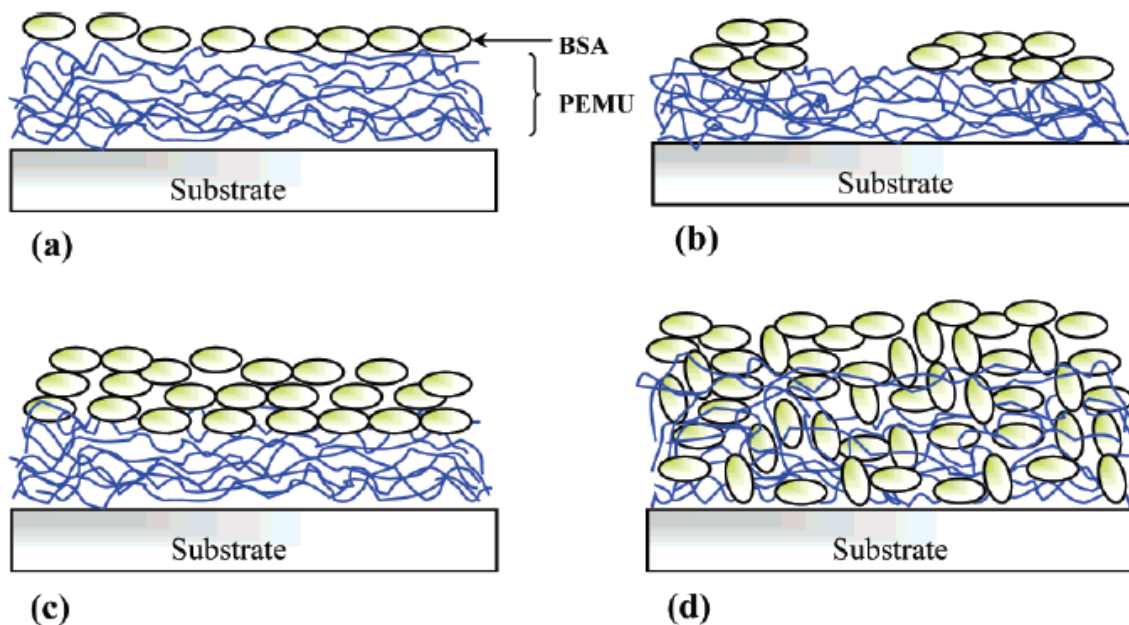


**Figure 1.4** Schematic of protein adsorption onto/into PEMs. Apparent monolayers (a and b), and apparent multilayers (c and d).<sup>55</sup> (Reprinted with permission from *Biomacromolecules* **2004**, 5, 1089. Copyright 2004 American Chemical Society.)

This thesis focuses on developing new PEMs as a platform for protein capture and immobilization. In particular, at physiological ionic strength, PEMs containing poly(acrylic acid) (PAA) exhibit minimal nonspecific adsorption of proteins, and activation of  $-\text{COOH}$  groups provides a means for covalent immobilization of antibodies and other proteins.<sup>55,59-61</sup> Moreover, these films also adsorb highly positively charged proteins such as lysozyme. However, improving binding capacity is still important in applications of these films for protein purification or immobilization. We hypothesized that LbL deposition of cylindrical, comb-like PAA might lead to thicker films with much greater binding capacities than corresponding multilayer films containing linear PAA.

#### 1.4. Grafted copolymers prepared by atom transfer radical polymerization (ATRP)

Grafted copolymers can be prepared via various strategies: homopolymerization of macromonomers ('grafting through'),<sup>62-66</sup> attachment of side chains to the backbone ('grafting to'),<sup>67-68</sup> and growth of side chains by polymerization from a macroinitiator ('grafting from').<sup>69-71</sup> Here we applied a 'grafting from' strategy via atom transfer radical polymerization (ATRP), which allows the control of length and molecular weight distribution of both the backbone and the side chains.

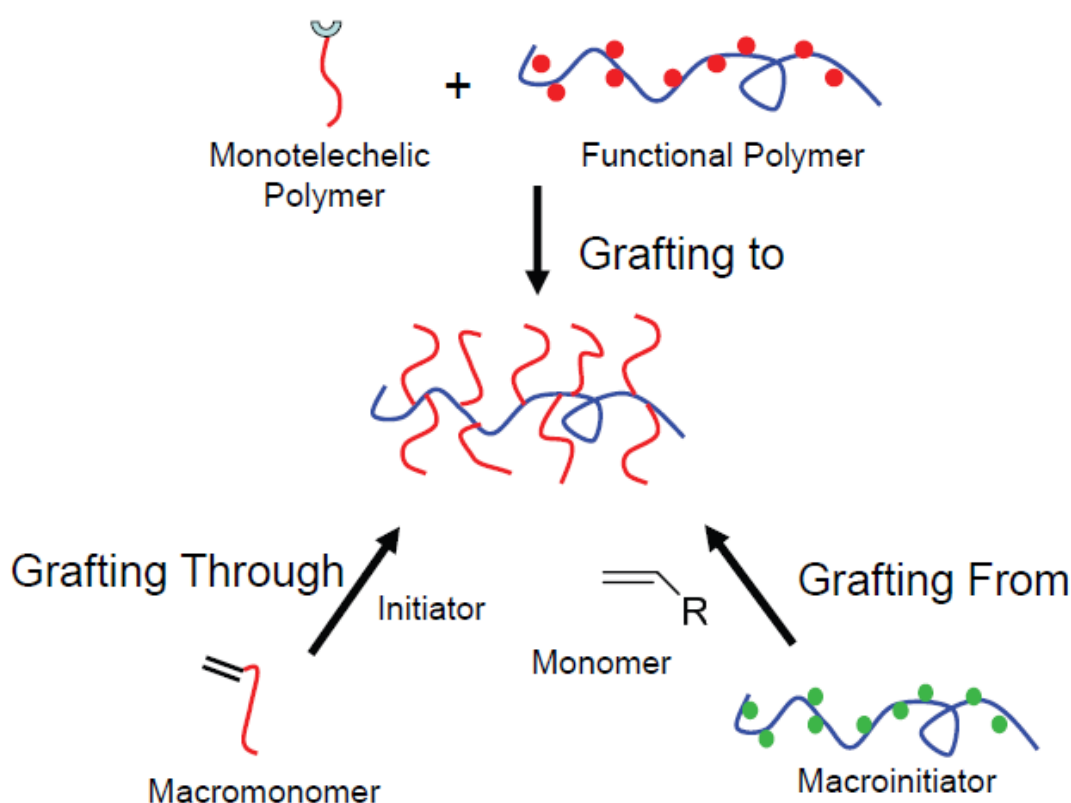
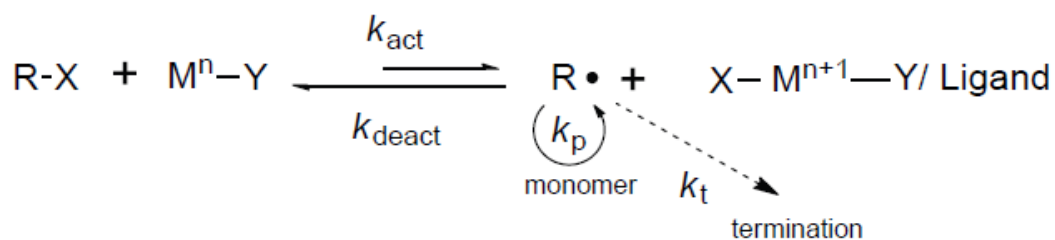


**Figure 1.5** Three main strategies for preparing grafted copolymers.

Since ATRP was first reported in 1995,<sup>72</sup> this method was widely developed to prepare various materials. A general mechanism is shown in Scheme 1.1.<sup>73</sup> Radicals are generated through a reversible redox process catalyzed by a transition metal complex which undergoes

a one electron oxidation with abstraction of a halogen atom from a dormant species. This process reduces the concentration of active radicals and termination, providing polymers with a narrow molecular weight distribution. The diminished termination rate makes ATRP attractive for synthesis of copolymers with controlled compositions and topologies.



**Scheme 1.1** Kinetic scheme of ATRP

Other controlled radical polymerization (CRP) methods, such as nitroxide-mediated polymerization (NMP) and reversible addition-fragmentation chain transfer polymerization (RAFT) have also attracted significant interest for preparing copolymers with complex architectures, and these methods have certain advantages and limitations.<sup>74</sup> ATRP initiators, transition metal catalysts, and ligands are commercial products, and various monomers have been successfully polymerized using ATRP, including styrenes, (meth)acrylates, (meth)acrylamides, dienes, acrylonitrile, and other monomers which contain substituents that stabilize the propagating radicals.<sup>73</sup> However, ATRP of acidic monomers is a challenging problem and usually requires protection or neutralization, and in industrial applications, the catalyst must be removed from the final product. For NMP, polymerization of both methacrylates and less reactive monomers is very challenging, and RAFT is incompatible with basic monomers and those with primary amino groups.

## 1.5. Research motivation and objectives

In this work, we applied poly(2-hydroxyethyl methacrylate)-*graft*-poly(acrylic acid) (PHEMA-*g*-PAA) as polyanions to form PEMs (Scheme 2). PHEMA provides a relatively hydrophilic backbone modified by densely grafted PAA. LbL deposition of this cylindrical polyanion will involve the same interaction as adsorption of linear PAA, but the cylindrical shape may lead to thicker films. Thicker surface layers, in particular, might lead to additional protein binding. Additionally, cylindrical polyelectrolyte layers might form a looser multilayer to improve the penetration of proteins into the bulk of the film.

In addition to examining differences between films containing PHEMA-*g*-PAA and PAA, we also aimed to investigate the effect of deposition pH on protein-binding properties of the films. Deposition of PAA films at pH 3 and below leads to free –COOH groups in the film, and subsequent immersion of these films into pH 7 buffer should deprotonate these groups to increase film swelling and create adsorption sites. In fact, as this work shows, the deposition pH has a much stronger effect on protein binding to PAA-containing films than the structure of the PAA, i.e. linear versus graft copolymer.

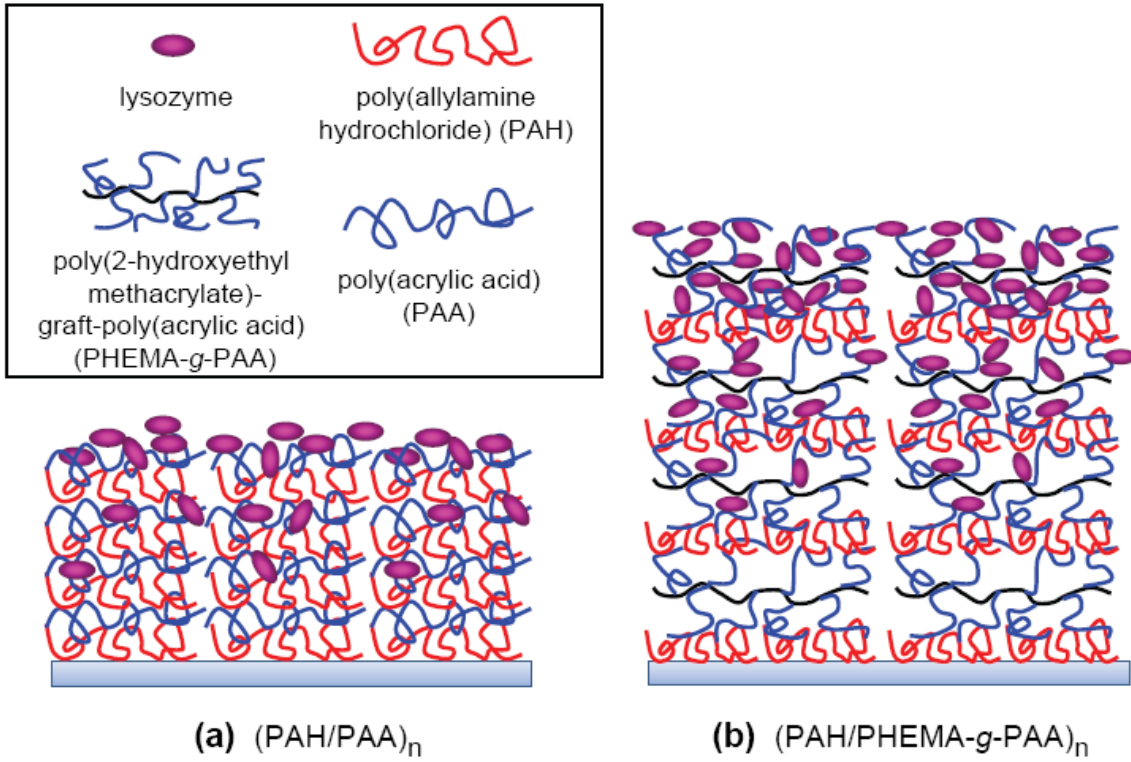


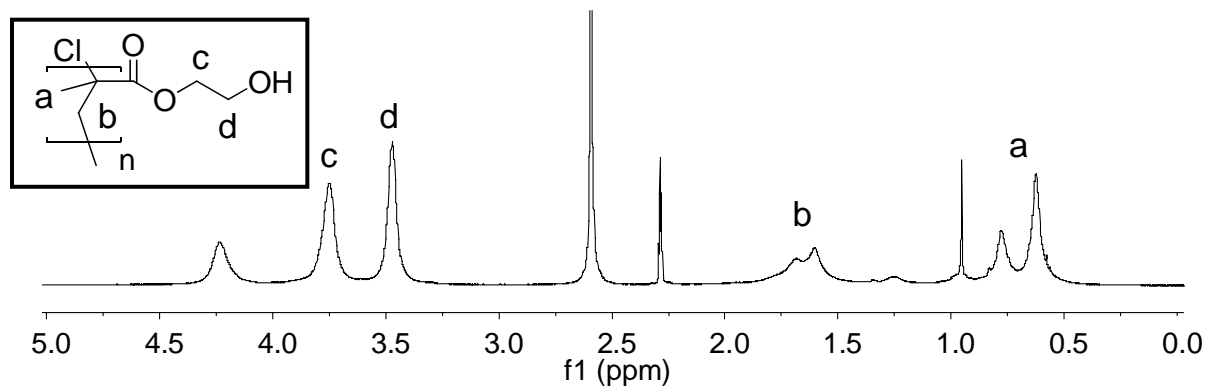
**Figure 1.6** Cross-section of layer-by-layer deposition of (a) linear polymers and (b) grafted polymers.

## Chapter 2

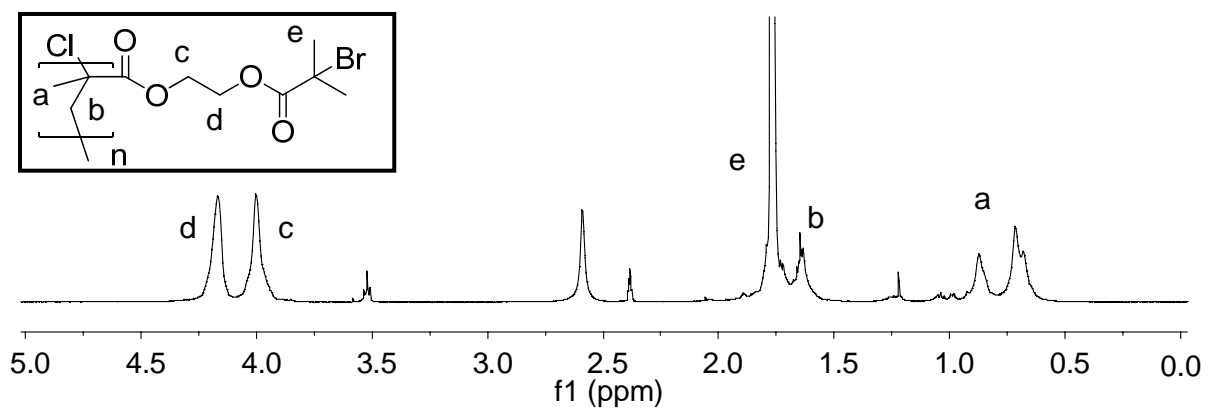
### Layer-by-layer deposition of PHEMA-*g*-PAA/PAH bilayers on Au substrates

#### 2.1 Synthesis of PHEMA-*g*-PAA

Synthesis of the grafted copolymer, PHEMA-*g*-PAA, proceeds in four steps (Scheme 2.1). Copper-catalyzed ATRP of HEMA gives linear PHEMA and subsequent esterification of PHEMA with 2-bromoisobutyryl bromide yields the macroinitiator, poly(2-(2-bromoisobutyryloxy)ethyl methacrylate) (PBIEM). <sup>1</sup>H NMR spectra indicate essentially 100% esterification (Figure 2.1). Based on GPC data ( $M_n = 119\,000$ ,  $M_w/M_n = 1.03$ , see Figure 2.2), PBIEM has an average degree of polymerization of 430.



(a)



(b)

**Figure 2.1**  $^1\text{H}$  NMR spectra of (a) PHEMA and (b) PBIEM in  $\text{CDCl}_3$  with 10%  $d^6$ -DMSO

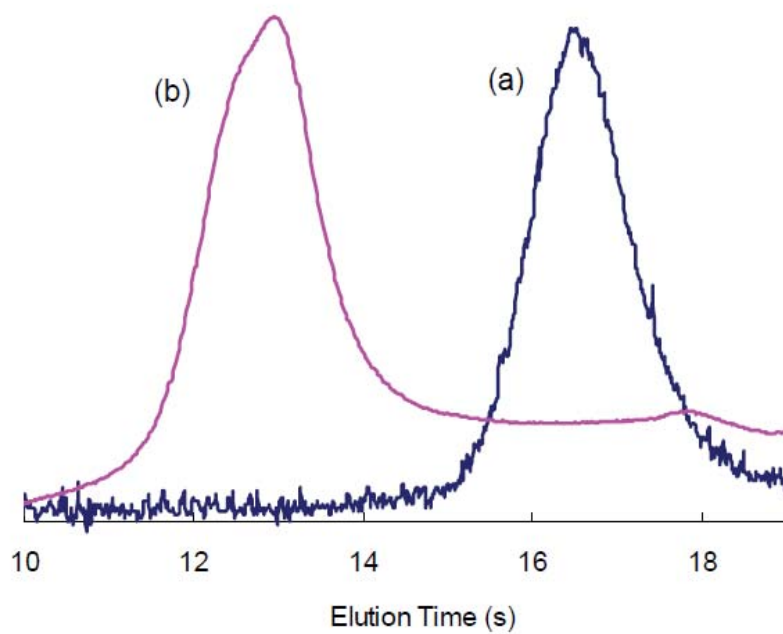
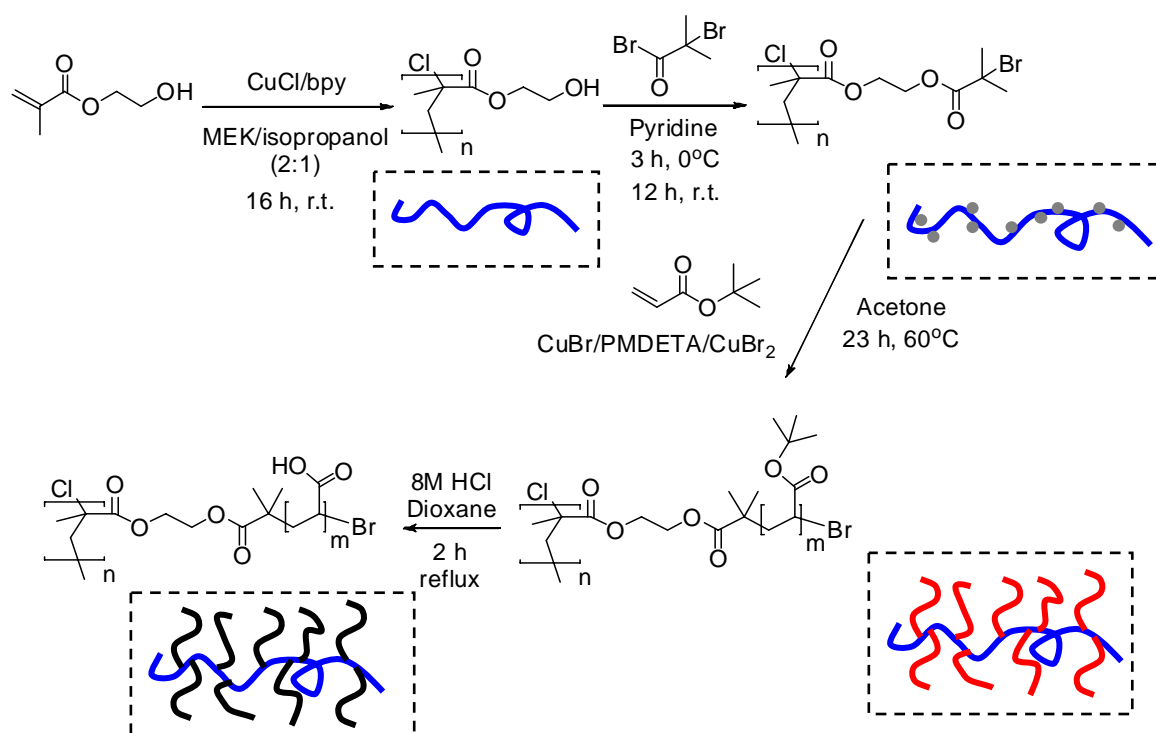


**Figure 2.2** Gel-permeation chromatograms of (a) PBIEM and (b) PHEMA-g-PtBA detected using a multi-angle light scattering detector.



**Scheme 2.1** Synthesis of poly(2-hydroxyethyl methacrylate)-*g*-poly(acrylic acid) (PHEMA-*g*-PAA)

Grafting *PtBA* from PBIEM also occurs via ATRP. GPC of the grafted copolymer shows a very high average molecular weight with a relatively narrow distribution ( $M_n = 7.99 \times 10^6$ ,  $M_w/M_n = 1.44$ , see Figure 2.2), indicating successful grafting of *PtBA* with reasonable control over the polymerization. The GPC data correspond to an average degree of polymerization of 140 for the *PtBA* side chains if we assume 100% initiation efficiency from PBIEM, which is consistent with reports of similar reactions.<sup>71</sup> Thus the  $M_n$  for each *PtBA* grafted chain is 61,500. Finally, deprotection of the *tert*-butyl groups of PHEMA-*g*-*PtBA* proceeds in refluxing dioxane with 8 M hydrochloric acid for 2h. The disappearance of the  $^1\text{H}$  NMR signal from the methyl protons of the *tBA* groups (1.35 ppm) confirms deprotection to PHEMA-*g*-PAA.

## 2.2 Formation of (PAH/PHEMA-*g*-PAA)<sub>n</sub> films

PHEMA-*g*-PAA chains can serve as extremely large, somewhat 3-dimensional polyanions in novel PEMs. Chemically, PHEMA-*g*-PAA should behave like linear PAA due to the high degree of polymerization of the PAA side chains. Literature reports show only a slightly higher  $pK_a$  value for star-shaped PAA than linear PAA.<sup>75-76</sup> However, the length of the PAA side chains in PHEMA-*g*-PAA is 1/3 of the PHEMA backbone, so the grafted copolymers should be somewhat cylindrical. Steric constraints due to interactions with neighboring side chains may lead to extended chains and more rapid film growth compared to PEMs with linear polymers or even star-like polymers<sup>77-79</sup> and dendrimers.<sup>80-84</sup> The high molecular weight of the grafted polymer might also increase the thickness of PEMs, although typically, molecular weight has a relatively small effect on polyelectrolyte adsorption.<sup>26,44,85</sup>

Figure 2.3 shows the ellipsometric thicknesses of (PAH/PHEMA-*g*-PAA)<sub>n</sub> and control (PAH/PAA)<sub>n</sub> films as a function of the number of bilayers (n) adsorbed from pH 7 solutions. After adsorption of the first two priming bilayers, the (PAH/PHEMA-*g*-PAA)<sub>n</sub> films grow much faster than (PAH/PAA)<sub>n</sub>. At pH 7, both the ionized PAA side chains in PHEMA-*g*-PAA and linear PAA will extend due to electrostatic repulsion. In the case of linear PAA, however, this likely leads to adsorption of thin films with chains extended parallel to the surface. In contrast, with PHEMA-*g*-PAA, adsorption might occur with either the backbone or the side chains parallel to the surface (or some intermediate orientation), but all orientations lead to thicker films at full surface coverage. Nevertheless, the highest increase in thickness on deposition of an additional PAH/PHEMA-*g*-PAA bilayer is <10 nm. Given the average degree of side-chain polymerization of 140, which corresponds to a fully

extended side-chain length of 35 nm (0.25 nm per repeat unit), bilayer thicknesses of 10 nm are well within reason. (Films with more than 10 bilayers were visibly rough, so we could not determine their ellipsometric thickness.)

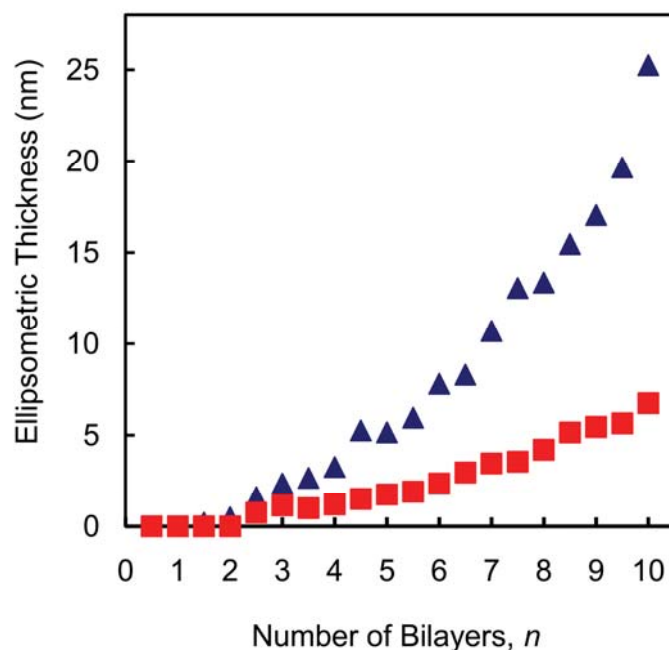


**Figure 2.3** Ellipsometric thicknesses of (PAH/PHEMA-*g*-PAA) $_n$  (triangles) and (PAH/PAA) $_n$  films (squares) deposited at pH=7 on Au substrates modified with a monolayer of MPA. The polyelectrolyte deposition solutions contained no NaCl. Integer numbers of bilayers indicate films terminated with PHEMA-*g*-PAA, and films with an extra half bilayer end in PAH.

Figure 2.3 suggests that the thickness of (PAH/PHEMA-*g*-PAA) $_n$  films increases exponentially with the number of bilayers, even though (PAH/PAA) $_n$  films show reasonably linear growth film both in this and other studies.<sup>48</sup> Previous research suggests that diffusion of polymer chains throughout the film leads to exponential growth,<sup>38,86</sup> and low polyelectrolyte molecular weights favor exponential increases in thickness.<sup>44</sup> However, the molecular weight of PHEMA-*g*-PAA (4500 kDa, calculated from the molecular weight of PHEMA-*g*-PtBA assuming complete hydrolysis) is much higher than that of linear PAA (90

kDa), Perhaps the extended side chains of PHEMA-*g*-PAA allow diffusion of PAH throughout the film.

Adsorption pH dramatically affects the thickness of (PAH/PAA)<sub>n</sub> films<sup>48-50</sup> and may have a similar effect on (PAH/PHEMA-*g*-PAA)<sub>n</sub> coatings. (PAH/PAA)<sub>5</sub> and (PAH/PHEMA-*g*-PAA)<sub>5</sub> films show similar trends in thickness as a function of adsorption pH (Figure 2.4). Comparable trends with greater overall thickness occur for PEMs with 10 bilayers (Figure 2.5). In the case of (PAH/PAA)<sub>n</sub> films, decreased ionization of PAA at pH values <7 and of PAH at pH values >7 lead to increases in film thickness as shown previously.<sup>49</sup> Less ionization presumably leads to polymer chains with more loops and tails, and hence, greater thickness. Additionally, lower charge densities on polymer chains may require deposition of more polymers to compensate the charge on the surface. The latter explanation might better explain why the thickness of (PAH/PHEMA-*g*-PAA)<sub>5</sub> films increases at low deposition pH because the grafted copolymer should be most extended and occupy the greatest volume at high degrees of ionization. At all deposition pH values, (PAH/PHEMA-*g*-PAA)<sub>5</sub> films are about twice as thick as (PAH/PAA)<sub>5</sub> films (Figure 2.4).

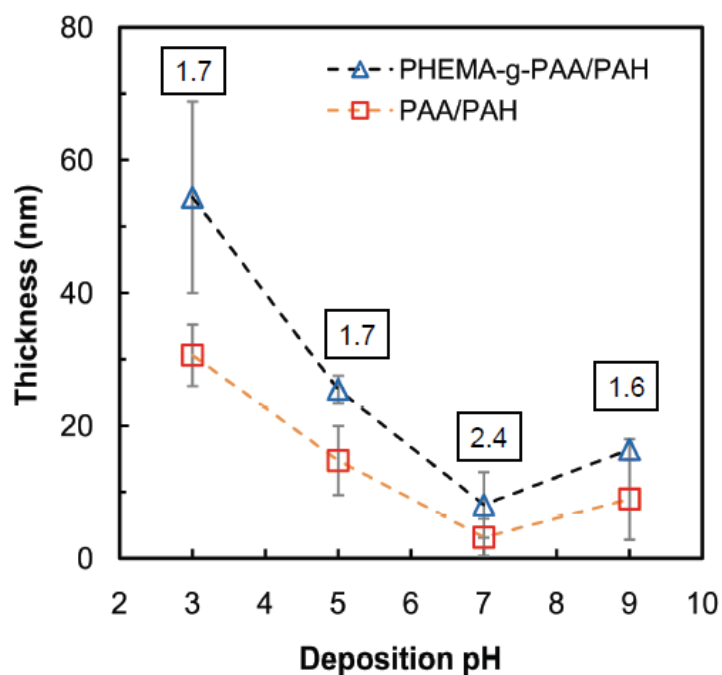


**Figure 2.4** Ellipsometric thicknesses of (PAH/PHEMA-*g*-PAA)<sub>5</sub> (triangles) and (PAH/PAA)<sub>5</sub> (squares) films deposited from solutions with various pH values and no supporting electrolyte. The numbers above the triangles represent the ratio of the average thicknesses of the two types of films deposited at the same pH. Data points are average of two trials and error bars here and below represents the difference of two trials.

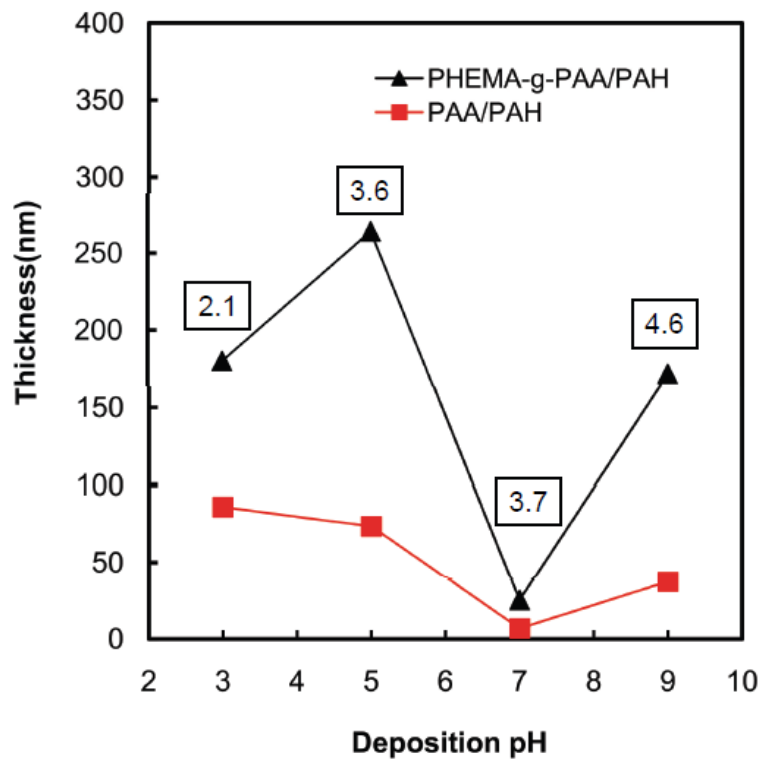


**Figure 2.5** Ellipsometric thicknesses of  $(\text{PAH/PHEMA-g-PAA})_{10}$  or  $(\text{PAH/PAA})_{10}$  films deposited from polyelectrolyte solutions with various pH values and no supporting electrolyte. Numbers in the figure represent the ratio of the  $(\text{PAH/PHEMA-g-PAA})_{10}$  and  $(\text{PAH/PAA})_{10}$  thicknesses.

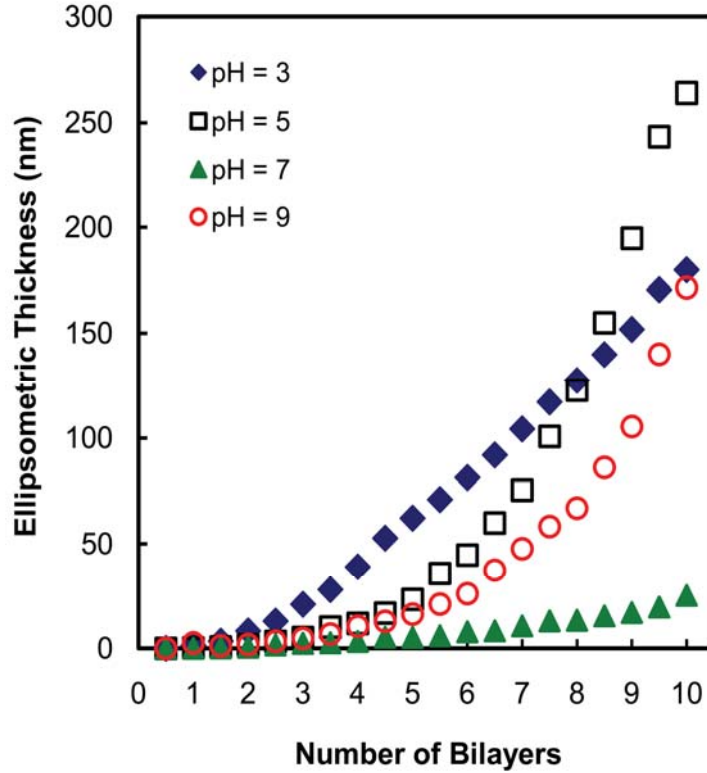
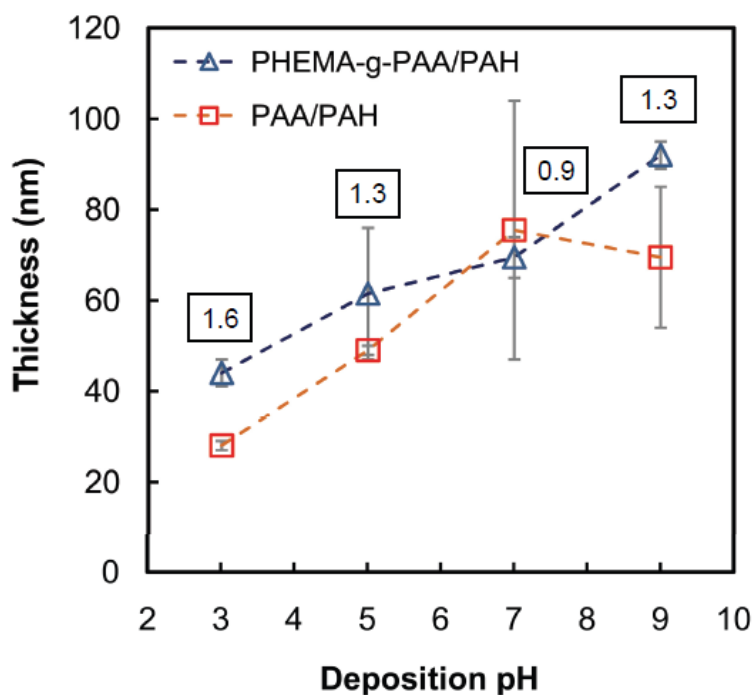


**Figure 2.6** Ellipsometric thicknesses of  $(\text{PAH/PHEMA-g-PAA})_n$  films deposited from polyelectrolyte solutions with various pH values and no supporting electrolyte. Integral bilayers indicate films terminated with PHEMA-g-PAA, and films with an extra half bilayer end in PAH.

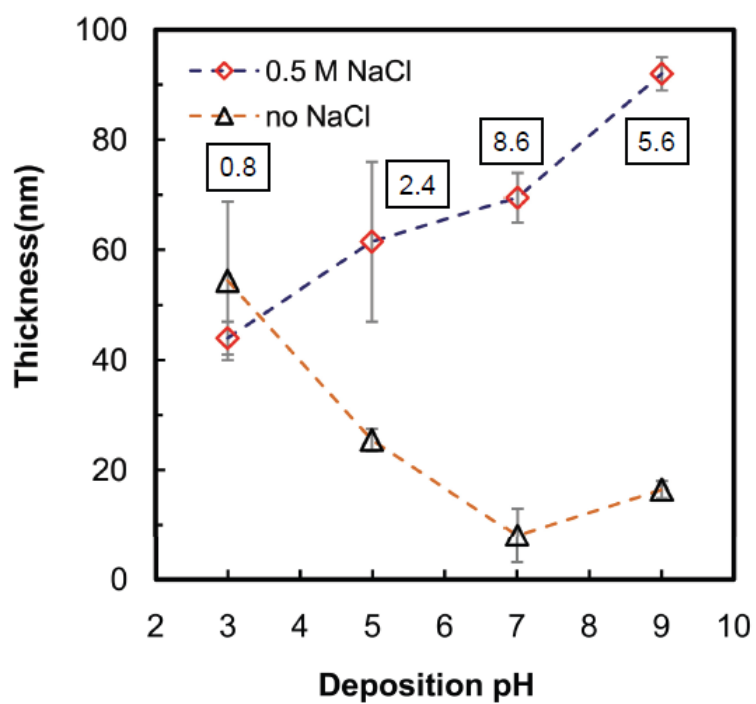
A number of studies show that adding salt to adsorption solutions increases the thickness and roughness of PEMs.<sup>32,39,50</sup> The excess electrolyte screens the charges along the polyelectrolyte chains to give more coiled chain conformations and thicker films.<sup>51</sup> Adding 0.5 M NaCl to PHEMA-g-PAA, PAA, and PAH deposition solutions dramatically changes trends in the thicknesses of  $(\text{PAH/PHEMA-g-PAA})_n$  and  $(\text{PAH/PAA})_n$  films as a function of pH (Figure 2.7). The thickness of these films increases essentially monotonically with solution pH, and the ratios of the thicknesses of  $(\text{PAH/PHEMA-g-PAA})_n$  and  $(\text{PAH/PAA})_n$  films deposited under the same conditions range from 0.9 to 1.6. At a deposition pH of 3, the supporting electrolyte has little effect on film thickness (compare Figures 2.6 and 2.7, see

Figure 2.8), but at all other adsorption pH values, film thicknesses increase by a factor between 2 and 9 when using 0.5 M NaCl in the deposition solution. The thickness increase in 0.5 M NaCl is especially large for (PAH/PAA)<sub>n</sub> films. Compensation of the polymer charge by ions in the electrolyte might result in a much more coiled conformation of linear polyelectrolytes, but have a less significant transformation on grafted PHEMA-*g*-PAA.

Overall, the presence of salt leads to thicker films in the absence of salt. However, rinsing of the films with 0.5 M NaCl rather than deionized water still leads to nonuniform films (Figure 2.9).



**Figure 2.7** Thickness of (PAH/PHEMA-*g*-PAA)<sub>5</sub> and (PAH/PAA)<sub>5</sub> multilayers deposited from polyelectrolyte solutions containing 0.5 M NaCl at various pH values. The numbers above the triangles represent the ratio of the average thicknesses of the two types of films deposited at the same pH.



**Figure 2.8** Ellipsometric thicknesses of (PAH/PHEMA-g-PAA)<sub>5</sub> multilayers deposited from polyelectrolyte solutions at various pH values in the presence and absence of 0.5 M NaCl.

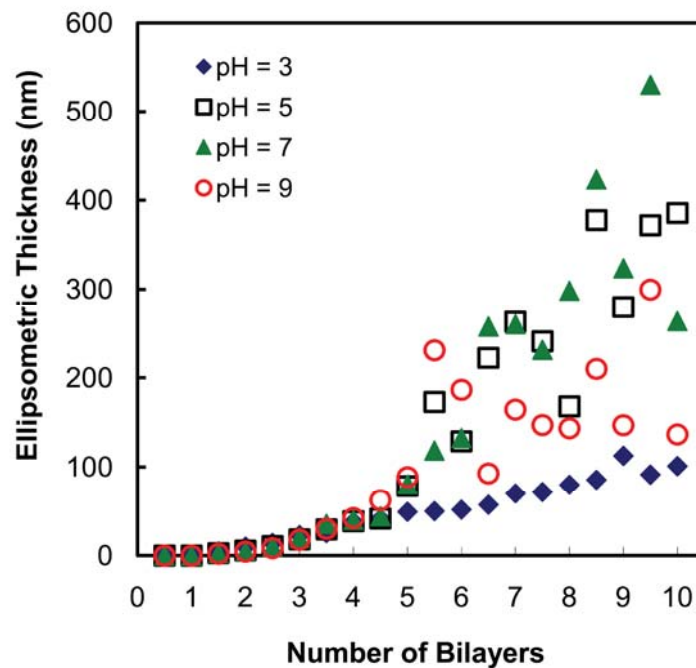


**Figure 2.9** Ellipsometric thicknesses of (PAH/PHEMA-*g*-PAA)<sub>*n*</sub> films deposited from polyelectrolyte solutions containing 0.5 M NaCl at various pH values. Integral bilayers indicate films terminated with PHEMA-*g*-PAA, and half bilayer films end in PAH. Films with more than 5 bilayers layers are relatively rough, so there is significant scatter in the ellipsometric results.

## Chapter 3

### Lysozyme Binding on (PAH/PHEMA-*g*-PAA)<sub>n</sub> and (PAH/PAA)<sub>n</sub> multilayers

Protein adsorption on PEMs is a simple method for creating functional thin films, both on flat surface and in membranes.<sup>20-25</sup> This study examines sorption of lysozyme, which is positively charged in pH 7.4 phosphate buffer (the isoelectric point of lysozyme is 11.4<sup>87</sup>), in (PAH/PHEMA-*g*-PAA)<sub>n</sub> and (PAH/PAA)<sub>n</sub> multilayers with the polyanion as the outermost layer. Initially, we thought that protein would adsorb primarily on the surface, and that the large size of PHEMA-*g*-PAA molecules would enhance protein binding. However, in some cases, sorption of proteins can occur throughout a PEM film to yield the equivalent of many monolayers of protein.<sup>55</sup>

#### 3.1 Lysozyme binding on (PAH/PHEMA-*g*-PAA)<sub>n</sub> and (PAH/PAA)<sub>n</sub> multilayers

##### deposited at various pH values

Initially, we examined lysozyme sorption from phosphate buffer (pH 7.4) into (PAH/PHEMA-*g*-PAA)<sub>5</sub> and (PAH/PAA)<sub>5</sub> films deposited from polyelectrolyte solutions with different pH values and no added supporting electrolyte. With the exception of films deposited at pH 3, all (PAH/PAA)<sub>5</sub> films sorb the equivalent of <5 nm of lysozyme (Figure 3.1). Thus, these films essentially adsorb a monolayer or less of lysozyme (14 600 Da, 3×3×4.5 nm)<sup>88</sup> on the surface. Strong ion-pairing in films deposited at pH values ≥5 likely prevents lysozyme from entering the film.<sup>48-50</sup> (PAH/PHEMA-*g*-PAA)<sub>5</sub> films deposited at

pH values  $\geq 5$  show 2-5-fold higher lysozyme sorption than corresponding (PAH/PAA)<sub>5</sub> coatings. This could be due to more binding in the thicker layer at surface or a somewhat looser film.

Both (PAH/PHEMA-*g*-PAA)<sub>5</sub> and (PAH/PAA)<sub>5</sub> deposited at pH 3 contain free COOH groups that deprotonate in the pH 7.4 buffer. These new carboxylate groups should provide lysozyme binding sites and increase film swelling to enhance diffusion of lysozyme into the film. Both (PAH/PHEMA-*g*-PAA)<sub>5</sub> and (PAH/PAA)<sub>5</sub> deposited at pH 3 bind an amount of lysozyme equivalent to the initial film thickness. These results are consistent with a surface plasmon resonance study that showed a 2-fold increase in lysozyme adsorption to PAH/PAA films deposited at pH 2.0 compared to films in which PAH was deposited at pH 7.5 and PAA was deposited at pH 3.5.<sup>59</sup> With deposition at pH 3 the (PAH/PHEMA-*g*-PAA)<sub>5</sub> shows 50% more lysozyme binding than (PAH/PAA)<sub>5</sub>, but this is likely due only to an increase in film thickness.

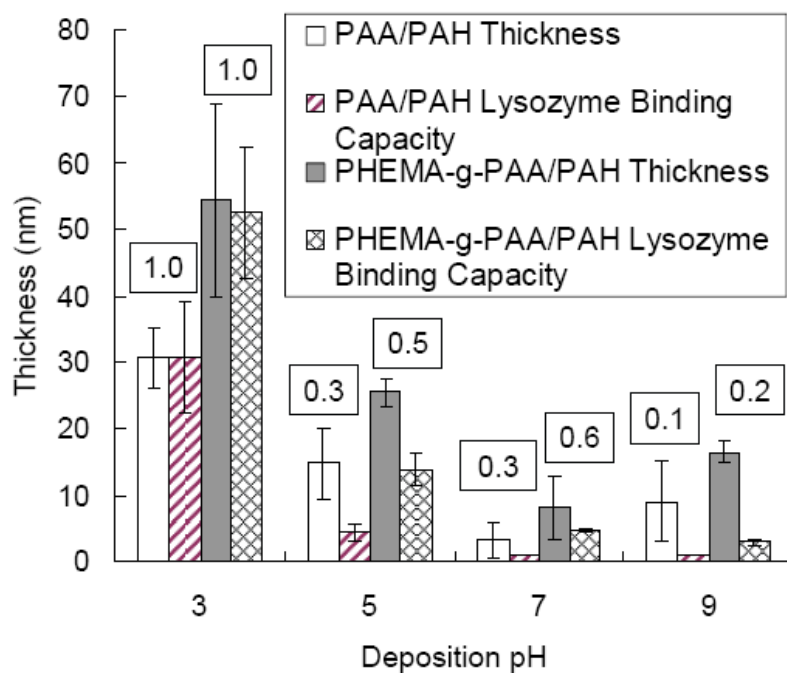


**Figure 3.1** Film thicknesses and the equivalent thickness of lysozyme sorbed in (PAH/PHEMA-g-PAA)<sub>5</sub> and (PAH/PAA)<sub>5</sub> multilayers deposited from polyelectrolyte solutions with various pH values and no supporting electrolyte. The numbers above the bars represent the ratios of the lysozyme equivalent thickness to the film thickness. The equivalent thickness is the thickness of spin-coated lysozyme that would give an FTIR absorbance equivalent to that of the sorbed lysozyme.

### 3.2 Lysozyme binding on (PAH/PHEMA-g-PAA)<sub>n</sub> and (PAH/PAA)<sub>n</sub> multilayers

#### deposited with a supporting electrolyte

Formation of (PAH/PHEMA-g-PAA)<sub>5</sub> and (PAH/PAA)<sub>5</sub> films from solutions containing 0.5 M NaCl greatly enhances lysozyme sorption, regardless of the pH used for film deposition (compare Figure 3.1 and 3.2). The (PAH/PHEMA-g-PAA)<sub>5</sub> and (PAH/PAA)<sub>5</sub> films deposited at pH 3 in 0.5 M NaCl show some of the highest lysozyme binding capacities, despite these films have the lowest thicknesses prior to lysozyme adsorption. Multilayer films deposited at pH 7 and pH 9 also bind remarkably large amounts of protein, suggesting that

these films either contain a larger number of intrinsic ion-exchange sites, or the lysozyme readily disrupts polyanion-polycation ion pairs to create adsorption sites.

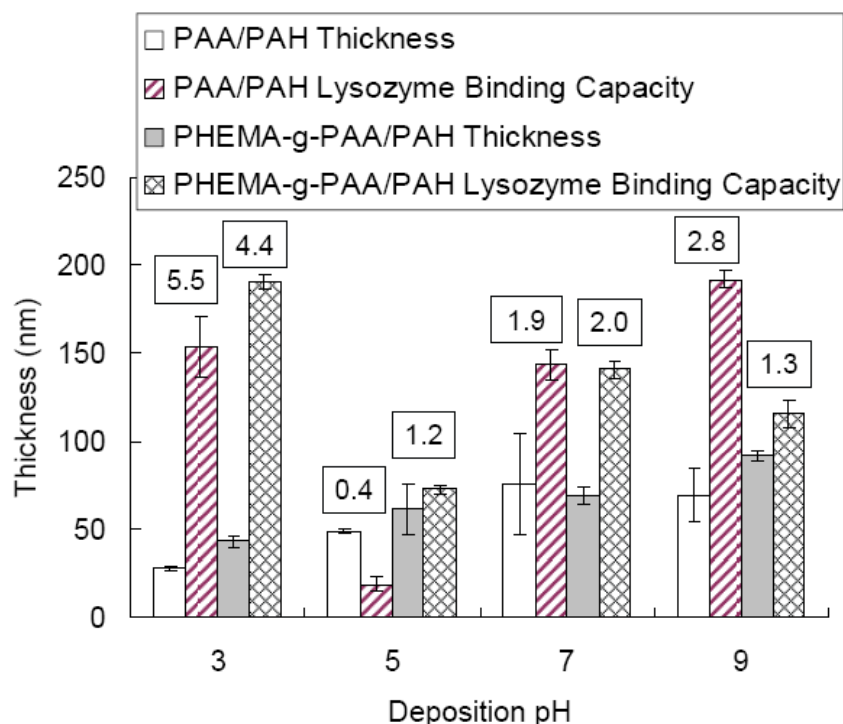


**Figure 3.2** Film thicknesses and the equivalent thickness of lysozyme sorbed in (PAH/PHEMA-g-PAA)<sub>5</sub> and (PAH/PAA)<sub>5</sub> multilayers deposited from polyelectrolyte solutions containing 0.5 M NaCl at various pH values. The numbers above the bars represent the ratios of the lysozyme equivalent thickness to the film thickness. The equivalent thickness is the thickness of spin-coated lysozyme that would give an FTIR absorbance equivalent to that of the sorbed lysozyme.

The relatively low sorption capacity of films prepared at pH 5 with 0.5 M NaCl may indicate that these films have the strongest intrinsic ion-pairing between cations and anions. Interestingly, only the film deposited at pH 5 shows significantly more binding to (PAH/PHEMA-g-PAA)<sub>5</sub> than (PAH/PAA)<sub>5</sub>. At this deposition pH, the graft copolymer may have a somewhat looser structure and more binding at the film surface.

### **3.3 Comparison of lysozyme binding capacities of (PAH/PHEMA-*g*-PAA)<sub>n</sub> and**

#### **(PAH/PAA)<sub>n</sub> multilayers**

Since PEMs deposited at pH 3 in 0.5 M NaCl clearly exhibit the highest ratio of bound lysozyme to film thickness (Figure 3.2), we examined binding to these coatings as a function of the number of layers in the film. For both (PAH/PHEMA-*g*-PAA)<sub>n</sub> and (PAH/PAA)<sub>n</sub>, the amount of adsorbed lysozyme increases with film thickness, but the ratio of lysozyme binding to film thickness decreases with the number of layers (Figure 3.3). This suggests that the accessibility of the film interior decreases somewhat with the addition of more layers. For the same number of layers, all (PAH/PHEMA-*g*-PAA)<sub>n</sub> films bind more lysozyme than (PAH/PAA)<sub>n</sub>. However, the ratios of lysozyme binding to film thickness are similar for these two polyelectrolyte systems. This result implies that the internal structure of (PAH/PHEMA-*g*-PAA)<sub>n</sub> multilayers is similar to the structure of (PAH/PAA)<sub>n</sub>.

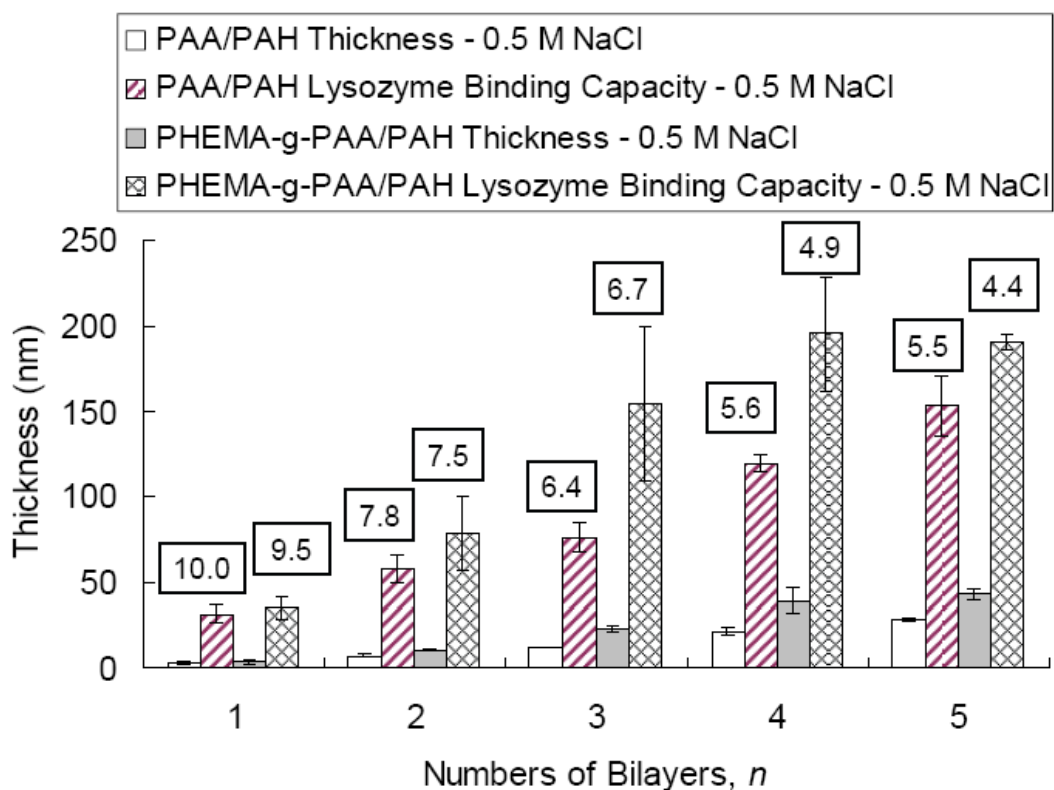
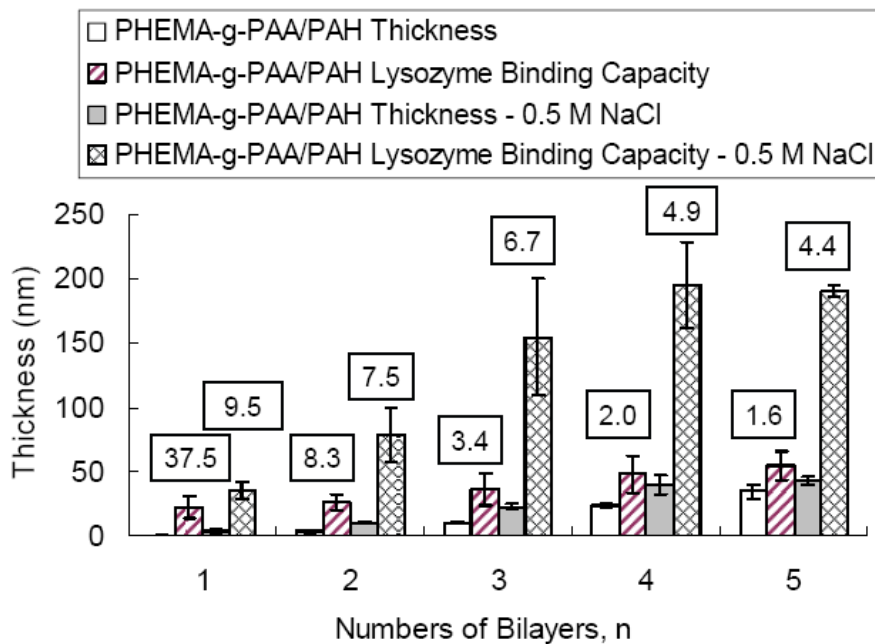
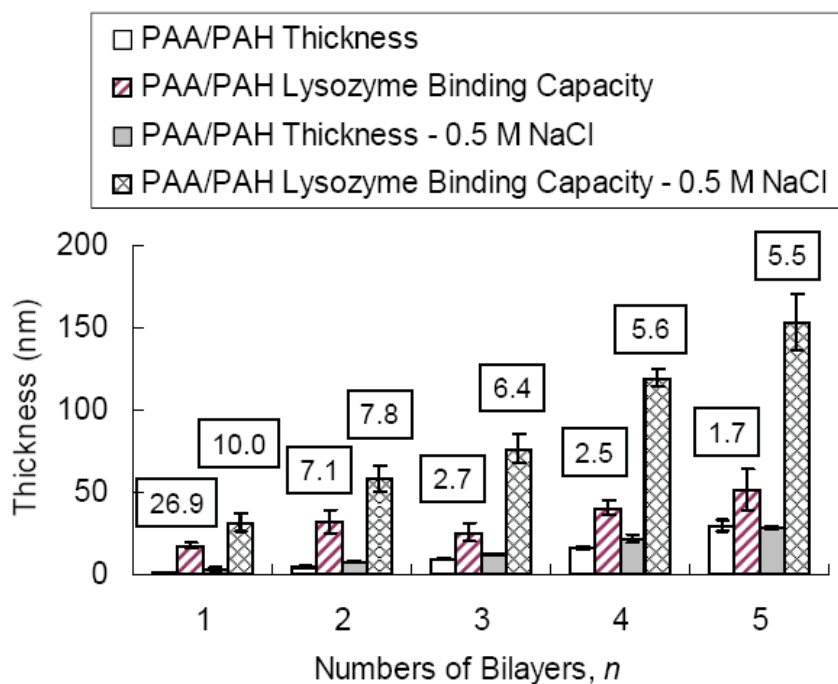


**Figure 3.3** Lysozyme binding capacities of  $(\text{PAH/PHEMA-g-PAA})_n$  or  $(\text{PAH/PAA})_n$  multilayers ( $n=1\sim 5$ ) deposited from polyelectrolyte solutions containing 0.5 M NaCl at pH=3. The numbers above the bars represent the ratios of the lysozyme equivalent thickness to the film thickness. The equivalent thickness is the thickness of spin-coated lysozyme that would give an FTIR absorbance equivalent to that of the sorbed lysozyme.



(a)



(b)

**Figure 3.4** Lysozyme binding capacities of (a)  $(\text{PAH/PHEMA-g-PAA})_n$  and (b)

$(\text{PAH/PAA})_n$  multilayers ( $n=1\sim5$ ) deposited from polyelectrolyte solutions at  $\text{pH}=3$  both in the presence and absence of  $0.5 \text{ M NaCl}$ . The numbers above the bars represent the ratios of the lysozyme equivalent thickness to the film thickness. The equivalent thickness is the thickness of spin-coated lysozyme that would give an FTIR absorbance equivalent to that of the sorbed lysozyme.

## Chapter 4

### Experimental

#### 4.1 Materials

Unless otherwise noted, all chemicals were obtained from Aldrich and used as received without further purification. 2,2-Bipyridine (bpy, 99%) was recrystallized from hexanes and sublimed prior to use. Triethylamine was distilled from calcium hydride under a nitrogen atmosphere and stored under nitrogen. 2-Hydroxyethyl methacrylate (HEMA) (98%) and *tert*-butyl acrylate (*t*BA) (98%), were passed through a column of activated basic alumina to remove inhibitors (length  $\times$  diameter: ca. 10 cm  $\times$  3 cm). Methyl ethyl ketone (MEK) and isopropanol were stored with 3 Å molecular sieves.

Poly(allyl amine hydrochloride) (PAH, molecular weight 120,000 ~ 200,000 Da) was purchased from Alfa Aesar, and poly(acrylic acid) (PAA, molecular weight 90 000 Da, 25 wt% solution in water) was obtained from Polysciences. Aqueous solutions of 0.02 M PAH, 0.01 M PAA and 0.005 M PHEMA-*g*-PAA were prepared in deionized water (18.2 MΩcm, Milli-Q), and pH values were adjusted with 0.1 M NaOH or HCl (polymer concentrations are given with respect to the repeating unit). Au-coated silicon wafers were prepared by electron-beam evaporation of 200 nm of Au on 20 nm of Cr on Si (100) wafers. Silicon (SiO<sub>2</sub> surface) and Au-coated wafers were cleaned in a UV/O<sub>3</sub> chamber for 15 min prior to use.

## 4.2 Preparation of poly(2-hydroxyethyl methacrylate)-*graft*-poly(acrylic acid)

### (PHEMA-*g*-PAA)

#### 4.2.1 ATRP of HEMA

Poly(2-hydroxyethyl methacrylate) (PHEMA) was prepared by ATRP using a modified literature procedure.<sup>89</sup> Ethyl 2-bromoisobutyrate (EBiB) (97 mg, 0.50 mmol) bpy (156 mg, 1.00 mmol), MEK (2 mL) isopropanol (1 mL) and HEMA (6.44 g, 6.0 mL, 50 mmol) were added to a 25 mL Schlenk flask, and degassed by three freeze-pump-thaw cycles. CuCl (50 mg, 0.50 mmol) was added under a flow of N<sub>2</sub>, and the mixture was stirred at room temperature for 16 h. The polymer solution was diluted in acetone/isopropanol (volume ratio 2:1) and passed through a basic alumina column. Evaporating the solvent gave the purified polymer. <sup>1</sup>H NMR (CDCl<sub>3</sub>, 10% *d*<sup>6</sup>-DMSO): δ = 3.87 (-CH<sub>2</sub>-OCO, s, 2H), 3.59 (-CH<sub>2</sub>-OH, s, 2H), 2.05-1.60 (-CH<sub>2</sub>-C, br, 2H), 0.89 (-CH<sub>3</sub>, s, 1H), 0.73 (-CH<sub>3</sub>, s, 2H) ppm.

#### 4.2.2 Preparation of macroinitiator, poly(2-(2-bromoisobutyryloxy)ethyl methacrylate) (PBIEM)<sup>71</sup>

During 60 min, α-bromoisobutyryl bromide (7.4 g, 32 mmol) was added dropwise to a 0 °C solution of PHEMA (2.0 g, 15 mmol of OH groups) in anhydrous pyridine (30 mL). The mixture was stirred for 3 h at 0 °C and then for 12 h at room temperature. The insoluble pyridinium salt was removed by filtration, and the solvent was removed by rotary evaporation. The crude polymer was dissolved in 10 mL THF and purified by precipitation into 250 mL methanol. Yield: 31 %. <sup>1</sup>H NMR (CDCl<sub>3</sub>, 10% *d*<sup>6</sup>-DMSO): δ = 4.17 (-CH<sub>2</sub>-OCO, s, 2H), 4.00 (-CH<sub>2</sub>-OCO, s, 2H), 1.77 (-C(Br)(CH<sub>3</sub>)<sub>2</sub>, s, 6H), 1.65 (-CH<sub>2</sub>-C, s, 2H), 0.87 (-CH<sub>3</sub>, s, 1H), 0.72 (-CH<sub>3</sub>, s, 2H) ppm.

### 4.2.3 Preparation of PHEMA-*g*-PtBA<sup>71</sup>

In a 25 mL Schlenk flask, PBIEM (0.23 g, 0.82 mmol 2-bromoisobutyryloxy groups), CuBr<sub>2</sub> (9 mg, 41 mmol), N,N,N',N',N''-pentamethyldiethylenetriamine (PMDETA) (150 g, 86 mmol), *t*BA (10.5 g, 12 mL, 82 mmol) and acetone (3 mL) were combined and degassed by three freeze-pump-thaw cycles. CuBr (0.118 g (0.82 mmol) was added under a flow of N<sub>2</sub>, and the mixture was stirred at 60 °C for 23 h. The resulting polymer was dissolved in acetone and purified by passage through a basic alumina column (to remove catalyst) and precipitation in water. <sup>1</sup>H NMR (CDCl<sub>3</sub>): δ = 2.36-2.07 (-CH<sub>2</sub>-C, br, 2H), 1.90-1.68 (-CH-COO*t*Bu, br, 1H), 1.47-1.20 (-OC(CH<sub>3</sub>)<sub>3</sub>, br, 9H) ppm.

### 4.2.4 Hydrolysis of PHEMA-*g*-PtBA to PHEMA-*g*-PAA<sup>90</sup>

In a 10 mL round bottom flask equipped with a condenser, a solution of PHEMA-*g*-PtBA (3.0 g, 23 mmol *tert*-butyl ester groups), dioxane (45 mL) and concentrated HCl (15 mL, 0.48 mol), was heated to reflux. After about 2 h, the solution was cooled, and the excess reagents were removed by evaporation under vacuum. <sup>1</sup>H NMR (D<sub>2</sub>O, pH>10 adjusted by NaOD): δ = 2.37-2.03 (-CH-COOH, br, 1H), 1.90-1.35 (-CH<sub>2</sub>-C, br, 2H) ppm.

## 4.3 Preparation of polyelectrolyte multilayer (PEM) films

Au-coated Si substrates (24 mm × 11 mm) were immersed in 5 mM 3-mercaptopropionic acid (MPA) in ethanol for 2 h, rinsed with ethanol and dried with N<sub>2</sub> to form a monolayer of MPA and create a negatively charged surface at neutral pH. Then the substrates were immersed in 0.02 M aqueous PAH, adjusted to the desired pH, for 5 min and subsequently rinsed with deionized water and blown dry with N<sub>2</sub>. Substrates were then immersed in a polyanion-containing solution (0.01 M PAA or PHEMA-*g*-PAA adjusted to the desired pH

value) for 5 min followed by the same rinsing and drying procedures. In some cases, the PAH and polyanion solutions also contained 0.5 M NaCl. The process was repeated to form multilayer films.

#### **4.4 Characterization of polymers and PEM films**

$^1\text{H}$  and  $^{13}\text{C}$  NMR analyses were carried out at room temperature on a Varian UnityPlus-500 spectrometer at 500 and 300 MHz, respectively, with the chemical shifts reported in ppm and referenced to signals from residual protons in the solvent.

Ellipsometric measurements were performed with a rotating analyzer ellipsometer (model M-44, J. A. Woollam) using WVASE32 software. The angle of incidence was  $75^\circ$ , and the film refractive index was assumed to be 1.500 for thickness calculations. Reflectance Fourier Transform Infrared (FTIR) spectroscopy was performed using a Nicolet 6700 FTIR spectrometer containing a PIKE grazing angle ( $80^\circ$ ) attachment. Spectra were typically collected with 128 scans using a UV/ozone-cleaned, Au-coated wafer as a background.

Polymer molecular weights were determined by gel permeation chromatography with multi angle light scattering detector (GPC-MALLS) at  $35^\circ\text{C}$  using two PLgel  $10\mu$  mixed-B columns in series (manufacturer-stated linear molecular weight range of  $500\text{-}10\times 10^6$  g/mol). The eluting solvent was THF at a flow rate of 1 mL/min. An Optilab rEX (Wyatt Technology Co.) refractive index detector and a DAWN EOS 18-angle light scattering detector (Wyatt Technology Co.) with a laser wavelength of 684 nm were used to calculate absolute molecular weights.

#### 4.5 Lysozyme binding

To immobilize lysozyme, substrates coated with PEM films were immersed in 1.0 mg/mL lysozyme in 20 mM phosphate buffer (pH 7.4) for 16 h at room temperature. Subsequently, these substrates were rinsed with 10 mL washing buffer (20 mM phosphate buffer containing 0.1% Tween-20 surfactant) and 10 mL water for 1 min each and dried with N<sub>2</sub>. The amount of lysozyme binding was determined by reflectance FTIR spectroscopy and express as the equivalent thickness of spin-coated lysozyme that would give the same absorbance.<sup>20</sup> The equivalent thickness  $d$  is calculated from the difference of absorbance ( $\Delta A$ ) at 1680 cm<sup>-1</sup> (amide band I of lysozyme) before and after binding lysozyme.  $d$  (nm) =  $\Delta A / 0.0017$ . Some of these thicknesses were confirmed using ellipsometry.

## References

## References

- (1) Jain, P.; Baker, G. L.; Bruening, M. L. *Annu. Rev. Anal. Chem.* **2009**, *2*, 387.
- (2) Barbey, R.; Lavanant, L.; Paripovic, D.; Schuwer, N.; Sugnaux, C.; Tugulu, S.; Klok, H. *A. Chem. Rev.* **2009**, *109*, 5437.
- (3) Bruening, M. L.; Dotzauer, D. M.; Jain, P.; Ouyang, L.; Baker, G. L. *Langmuir* **2008**, *24*, 7663.
- (4) Bunsow, J.; Kelby, T. S.; Huck, W. T. S. *Accounts Chem. Res.* **2010**, *43*, 466.
- (5) Edmondson, S.; Osborne, V. L.; Huck, W. T. S. *Chem. Soc. Rev.* **2004**, *33*, 14.
- (6) Zhao, B.; Brittain, W. J. *Prog. Polym. Sci.* **2000**, *25*, 677.
- (7) Boudou, T.; Crouzier, T.; Ren, K. F.; Blin, G.; Picart, C. *Adv. Mater.* **2010**, *22*, 441.
- (8) De Geest, B. G.; Sanders, N. N.; Sukhorukov, G. B.; Demeester, J.; De Smedt, S. C. *Chem. Soc. Rev.* **2007**, *36*, 636.
- (9) Tang, Z. Y.; Wang, Y.; Podsiadlo, P.; Kotov, N. A. *Adv. Mater.* **2006**, *18*, 3203.
- (10) Jaber, J. A.; Schlenoff, J. B. *Curr. Opin. Colloid Interface Sci.* **2006**, *11*, 324.
- (11) Hammond, P. T. *Adv. Mater.* **2004**, *16*, 1271.
- (12) Bertrand, P.; Jonas, A.; Laschewsky, A.; Legras, R. *Macromol. Rapid Commun.* **2000**, *21*, 319.
- (13) Decher, G. *Science* **1997**, *277*, 1232.
- (14) Decher, G.; Hong, J. D.; Schmitt, J. *Thin Solid Films* **1992**, *210*, 831.
- (15) Iler, R. K. *J. Colloid Interface Sci.* **1966**, *21*, 569.
- (16) Johnston, A. P. R.; Cortez, C.; Angelatos, A. S.; Caruso, F. *Curr. Opin. Colloid Interface Sci.* **2006**, *11*, 203.
- (17) Kidambi, S.; Bruening, M. L. *Chem. Mat.* **2005**, *17*, 301.
- (18) Kidambi, S.; Dai, J. H.; Li, J.; Bruening, M. L. *J. Am. Chem. Soc.* **2004**, *126*, 2658.
- (19) Quinn, J. F.; Johnston, A. P. R.; Such, G. K.; Zelikin, A. N.; Caruso, F. *Chem. Soc. Rev.* **2007**, *36*, 707.

- (20) Dai, J. H.; Baker, G. L.; Bruening, M. L. *Anal. Chem.* **2006**, *78*, 135.
- (21) Datta, S.; Cecil, C.; Bhattacharyya, D. *Ind. Eng. Chem. Res.* **2008**, *47*, 4586.
- (22) Jain, P.; Vyas, M. K.; Geiger, J. H.; Baker, G. L.; Bruening, M. L. *Biomacromolecules* **2010**, *11*, 1019.
- (23) Liu, G. Q.; Dotzauer, D. M.; Bruening, M. L. *J. Membr. Sci.* **2010**, *354*, 198.
- (24) Liu, J. J.; Yan, Y. F.; Yao, P. *Chin. J. Polym. Sci.* **2011**, *29*, 397.
- (25) Smuleac, V.; Butterfield, D. A.; Bhattacharyya, D. *Langmuir* **2006**, *22*, 10118.
- (26) Porcel, C. H.; Izquierdo, A.; Ball, V.; Decher, G.; Voegel, J. C.; Schaaf, P. *Langmuir* **2005**, *21*, 800.
- (27) Fukao, N.; Kyung, K. H.; Fujimoto, K.; Shiratori, S. *Macromolecules* **2011**, *44*, 2964.
- (28) Izquierdo, A.; Ono, S. S.; Voegel, J. C.; Schaaf, P.; Decher, G. *Langmuir* **2005**, *21*, 7558.
- (29) Krogman, K. C.; Zacharia, N. S.; Schroeder, S.; Hammond, P. T. *Langmuir* **2007**, *23*, 3137.
- (30) Ono, S. S.; Decher, G. *Nano Lett.* **2006**, *6*, 592.
- (31) US Patent 6, 926 B2, 2005; filed 2003.
- (32) Schlenoff, J. B.; Dubas, S. T. *Macromolecules* **2001**, *34*, 592.
- (33) Wang, F.; Ma, N.; Chen, Q. X.; Wang, W. B.; Wang, L. Y. *Langmuir* **2007**, *23*, 9540.
- (34) Sukhishvili, S. A.; Granick, S. *Macromolecules* **2002**, *35*, 301.
- (35) Guyomard, A.; Muller, G.; Glinel, K. *Macromolecules* **2005**, *38*, 5737.
- (36) Caruso, F.; Niikura, K.; Furlong, D. N.; Okahata, Y. *Langmuir* **1997**, *13*, 3422.
- (37) Picart, C.; Ladam, G.; Senger, B.; Voegel, J. C.; Schaaf, P.; Cuisinier, F. J. G.; Gergely, C. *J. Chem. Phys.* **2001**, *115*, 1086.
- (38) Hoda, N.; Larson, R. G. *J. Phys. Chem. B* **2009**, *113*, 4232.
- (39) McAloney, R. A.; Sinyor, M.; Dudnik, V.; Goh, M. C. *Langmuir* **2001**, *17*, 6655.
- (40) Salomaki, M.; Vinokurov, I. A.; Kankare, J. *Langmuir* **2005**, *21*, 11232.
- (41) Dubas, S. T.; Schlenoff, J. B. *Macromolecules* **1999**, *32*, 8153.

- (42) Richert, L.; Lavalle, P.; Payan, E.; Shu, X. Z.; Prestwich, G. D.; Stoltz, J. F.; Schaaf, P.; Voegel, J. C.; Picart, C. *Langmuir* **2004**, *20*, 448.
- (43) Porcel, C.; Lavalle, P.; Decher, G.; Senger, B.; Voegel, J. C.; Schaaf, P. *Langmuir* **2007**, *23*, 1898.
- (44) Sun, B.; Jewell, C. M.; Fredin, N. J.; Lynn, D. M. *Langmuir* **2007**, *23*, 8452.
- (45) Kujawa, P.; Moraille, P.; Sanchez, J.; Badia, A.; Winnik, F. M. *J. Am. Chem. Soc.* **2005**, *127*, 9224.
- (46) Buscher, K.; Graf, K.; Ahrens, H.; Helm, C. A. *Langmuir* **2002**, *18*, 3585.
- (47) Tan, H. L.; McMurdo, M. J.; Pan, G. Q.; Van Patten, P. G. *Langmuir* **2003**, *19*, 9311.
- (48) Bieker, P.; Schonhoff, M. *Macromolecules* **2010**, *43*, 5052.
- (49) Shiratori, S. S.; Rubner, M. F. *Macromolecules* **2000**, *33*, 4213.
- (50) Yoo, D.; Shiratori, S. S.; Rubner, M. F. *Macromolecules* **1998**, *31*, 4309.
- (51) von Klitzing, R. *Phys. Chem. Chem. Phys.* **2006**, *8*, 5012.
- (52) Nolte, A. J.; Takane, N.; Hindman, E.; Gaynor, W.; Rubner, M. F.; Cohen, R. E. *Macromolecules* **2007**, *40*, 5479.
- (53) Gergely, C.; Bahi, S.; Szalontai, B.; Flores, H.; Schaaf, P.; Voegel, J. C.; Cuisinier, F. J. G. *Langmuir* **2004**, *20*, 5575.
- (54) Hamada, K.; Yamashita, K.; Serizawa, T.; Kitayama, T.; Akashi, M. *J. Polym. Sci. Pol. Chem.* **2003**, *41*, 1807.
- (55) Salloum, D. S.; Schlenoff, J. B. *Biomacromolecules* **2004**, *5*, 1089.
- (56) Ladam, G.; Schaaf, P.; Cuisinier, F. J. G.; Decher, G.; Voegel, J. C. *Langmuir* **2001**, *17*, 878.
- (57) Ladam, G.; Schaaf, P.; Decher, G.; Voegel, J. C.; Cuisinier, F. J. G. *Biomol. Eng.* **2002**, *19*, 273.
- (58) Muller, M.; Rieser, T.; Dubin, P. L.; Lunkwitz, K. *Macromol. Rapid Commun.* **2001**, *22*, 390.
- (59) Mendelsohn, J. D.; Yang, S. Y.; Hiller, J.; Hochbaum, A. I.; Rubner, M. F. *Biomacromolecules* **2003**, *4*, 96.
- (60) Czeslik, C.; Jackler, G.; Hazlett, T.; Gratton, E.; Steitz, R.; Wittemann, A.; Ballauff, M. *Phys. Chem. Chem. Phys.* **2004**, *6*, 5557.

- (61) Jackler, G.; Wittemann, A.; Ballauff, M.; Czeslik, C. *Spectr.-Int. J.* **2004**, *18*, 289.
- (62) Tsukahara, Y.; Tsutsumi, K.; Yamashita, Y.; Shimada, S. *Macromolecules* **1990**, *23*, 5201.
- (63) O'Donnell, P. M.; Brzezinska, K.; Powell, D.; Wagener, K. B. *Macromolecules* **2001**, *34*, 6845.
- (64) Wintermantel, M.; Gerle, M.; Fischer, K.; Schmidt, M.; Wataoka, I.; Urakawa, H.; Kajiwara, K.; Tsukahara, Y. *Macromolecules* **1996**, *29*, 978.
- (65) Djalali, R.; Hugenberg, N.; Fischer, K.; Schmidt, M. *Macromol. Rapid Commun.* **1999**, *20*, 444.
- (66) Yamada, K.; Miyazaki, M.; Ohno, K.; Fukuda, T.; Minoda, M. *Macromolecules* **1999**, *32*, 290.
- (67) Ruokolainen, J.; Saariaho, M.; Ikkala, O.; ten Brinke, G.; Thomas, E. L.; Torkkeli, M.; Serimaa, R. *Macromolecules* **1999**, *32*, 1152.
- (68) Schappacher, M.; Deffieux, A. *Macromolecules* **2000**, *33*, 7371.
- (69) Beers, K. L.; Gaynor, S. G.; Matyjaszewski, K.; Sheiko, S. S.; Moller, M. *Macromolecules* **1998**, *31*, 9413.
- (70) Borner, H. G.; Beers, K.; Matyjaszewski, K.; Sheiko, S. S.; Moller, M. *Macromolecules* **2001**, *34*, 4375.
- (71) Cheng, G. L.; Boker, A.; Zhang, M. F.; Krausch, G.; Muller, A. H. E. *Macromolecules* **2001**, *34*, 6883.
- (72) Wang, J. S.; Matyjaszewski, K. *J. Am. Chem. Soc.* **1995**, *117*, 5614.
- (73) Matyjaszewski, K.; Xia, J. H. *Chem. Rev.* **2001**, *101*, 2921.
- (74) Matyjaszewski, K.; Tsarevsky, N. V. *Nat. Chem.* **2009**, *1*, 276.
- (75) Plamper, F. A.; Becker, H.; Lanzendorfer, M.; Patel, M.; Wittemann, A.; Ballauff, M.; Muller, A. H. E. *Macromol. Chem. Phys.* **2005**, *206*, 1813.
- (76) Wolterink, J. K.; van Male, J.; Stuart, M. A. C.; Koopal, L. K.; Zhulina, E. B.; Borisov, O. V. *Macromolecules* **2002**, *35*, 9176.
- (77) Connal, L. A.; Li, Q.; Quinn, J. F.; Tjipto, E.; Caruso, F.; Qiao, G. G. *Macromolecules* **2008**, *41*, 2620.
- (78) Kim, B. S.; Gao, H. F.; Argun, A. A.; Matyjaszewski, K.; Hammond, P. T. *Macromolecules* **2009**, *42*, 368.

- (79) Choi, I.; Suntivich, R.; Pamper, F. A.; Synatschke, C. V.; Muller, A. H. E.; Tsukruk, V. V. *J. Am. Chem. Soc.* **2011**, *133*, 9592.
- (80) Kim, B. Y.; Bruening, M. L. *Langmuir* **2003**, *19*, 94.
- (81) Tsukruk, V. V. *Adv. Mater.* **1998**, *10*, 253.
- (82) Tsukruk, V. V.; Rinderspacher, F.; Bliznyuk, V. N. *Langmuir* **1997**, *13*, 2171.
- (83) He, J. A.; Valluzzi, R.; Yang, K.; Dolukhanyan, T.; Sung, C. M.; Kumar, J.; Tripathy, S. K.; Samuelson, L.; Balogh, L.; Tomalia, D. A. *Chem. Mat.* **1999**, *11*, 3268.
- (84) Khopade, A. J.; Caruso, F. *Nano Lett.* **2002**, *2*, 415.
- (85) Losche, M.; Schmitt, J.; Decher, G.; Bouwman, W. G.; Kjaer, K. *Macromolecules* **1998**, *31*, 8893.
- (86) Picart, C.; Mutterer, J.; Richert, L.; Luo, Y.; Prestwich, G. D.; Schaaf, P.; Voegel, J. C.; Lavalle, P. *Proc. Natl. Acad. Sci. U. S. A.* **2002**, *99*, 12531.
- (87) Righetti, P. G.; Caravaggio, T. *Journal of Chromatography* **1976**, *127*, 1.
- (88) Blake, C. C. F.; Koenig, D. F.; Mair, G. A.; North, A. C. T.; Phillips, D. C.; Sarma, V. R. *Nature* **1965**, *206*, 757.
- (89) Beers, K. L.; Boo, S.; Gaynor, S. G.; Matyjaszewski, K. *Macromolecules* **1999**, *32*, 5772.
- (90) Davis, K. A.; Matyjaszewski, K. *Macromolecules* **2000**, *33*, 4039.